Magnitude of Catastrophic Thaw Lake Drainage and Influence on Arctic River Channel Morphology, Yukon Coastal Plain, Western Canadian Arctic

David W. Gardner

Bachelor of Science Honours Thesis

Supervisor: Dr. Lawrence Plug

Dalhousie University

Keywords: Thaw Lakes, Arctic Rivers, Permafrost, Lake Drainage, Channel Initiation

Dalhousie University

Department of Earth Sciences
Halifax, Nova Scotia
Canada B3H 3J5
(902) 494-2358
FAX (902) 494-6889

DATE: April 29 / 2005

AUTHOR: David William Gardner

TITLE: Magnitude of Catastrophic Thaw Lake Drainage and Influences on Arctic River Channel Morphology, Yukon Coastal Pain, Western Canadian Arctic

Degree: B. Sc. Convocation: Dec. 2005 Year: 2005

Abstract:

I hypothesize that the morphology and evolution of low-order stream channels in lowland permafrost regions are principally shaped by short-lived, massive floods that occur when thaw lakes drain. Thaw lakes, which form by thawing and collapse of ice-rich frozen ground, are known to drain into other lakes or river channels and tributaries. The imprint of thousands of drained basins on these landscapes underscores the possible importance of these events to stream channels. However, the influence of floods on channel and valley morphology has been poorly examined to date. To investigate these effects I use dual frequency differential GPS measurements (accurate to within +/- 5 cm) of valley and drained basin morphology from lower order drainage basins within the Running River watershed, Yukon Coastal Plain, Canada. The region is characterized by continuous permafrost (MAAT = -10 ℃) and extensive thaw lake development. Floods from a recently drained thaw lake with water volume of approximately 6.4 x 10^6 m^3 drained in two events (4.8 x 10^6 m^3 and 1.7 x 10^6 m^3 respectively) lasting approximately 0.5 to 2 days each, incised an approximately 15 m deep and up to 18 m wide and 500 m long channel. In comparison, maximum limit to flood volume from spring melt is 4 x 10^5 m^3, assuming instantaneous melt of snow pack in the entire drainage basin an order of magnitude in difference the measured drained thaw lake. GPS measurements show large flood terraces and deep incision of the current channel on Grayling Creek, a tributary to the Running River with baseflow of approximately 4 m^3/s. Sedimentary sections in flood terraces reveal numerous Holocene flood deposits. Massively over-fit river valleys are unlikely to have have been incised by the small amount of precipitation and melt water run-off that occur in the dry climate of the western Arctic. Thaw lake drainage events produce 20 to 100 times greater discharge (110.7 m^3/s) and 2 to 5 times greater stream power per unit width of channel (101.8 J/s). Stream power during thaw lake drainage events cause channel initiation to take place, where the active layer composed of permeable peat is over saturated allowing open flow to take place. Once open flow has been established, stream power causes large rates of rapid incision through the active layer and into the permafrost. Thaw lake drainage has a large affect on river channel morphology and acts as a primary architect in shaping low to intermediate order Arctic rivers and landscapes.

Acknowledgements:

The composition of this thesis has involved funding from the Polar Continental Shelf Project and NSERC for field work. GPS and computing equipment was supported by the Canadian Foundation for Innovation and Leica Geosystems. Thank you to my supervisor Lawrence Plug, for allowing me to travel to the Yukon Coastal Plain and work as a field assistant, and for aiding me through out the 2004/2005 school year during the writing of this thesis. He has inspired me to look at life and the earth in different ways, and for that I thank him. I would also like to thank Adam Mawer, my partner in crime, having him in the lab made work more amusing. I would like to thank Jennifer McIntosh, Carl Hemlick, and Sakalema Sikaneta for helping me brainstorm through some computing and theory related problems. I finally would like to thank my family, Mum and Dad, as well as my sister Victoria, and my girlfriend Jenn for always listening to me babble on about geology.

Table of Contents:

List of Figures:

List of Tables:

Chapter 1: General Introduction

Thaw lakes are water-filled topographic depressions found in continuous permafrost regions and are a dominant process shaping Arctic lowland and coastal environments. Disturbances in the thermal regime cause initial melting of permafrost to occur, resulting in thaw lake formation. Lake expansion occurs due to thermal heating of lakes via solar radiation causing ice-rich permafrost at lake margins to melt, collapse and subside. Thaw lake terrains are riddled with full, partly full, and drained basins. Two contrasting models explain the presence of drained thaw lake basins (French 1996). The

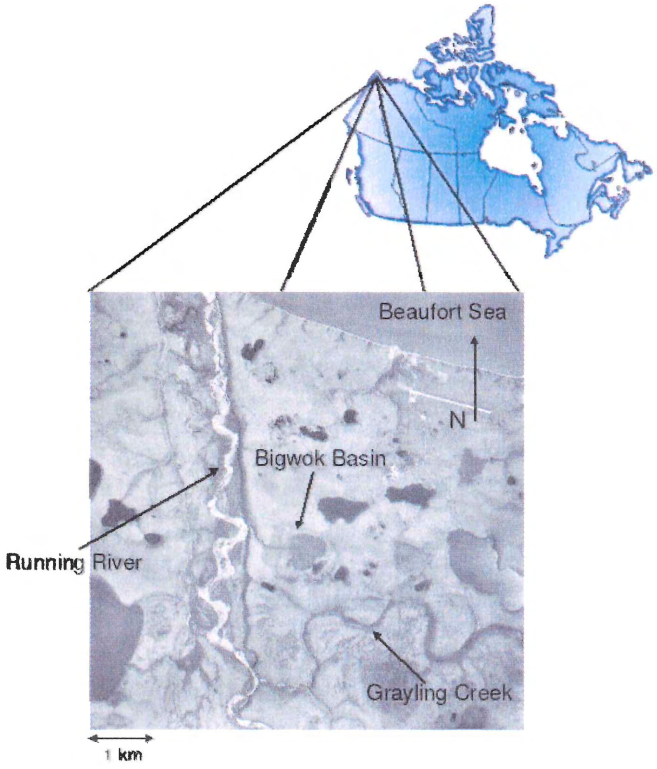

Figure 1.1 Air photo (NAPL 1985) indicating main aspects of the study area on the Yukon Coastal Plain

first attributes dry basins to gradual infilling and sedimentation--but this is unlikely because the thaw processes that release sediment are responsible for lake growth. The second attributes dry basins to catastrophic drainage following a tapping of a topographic low such as a river channel or tributary by expanding thaw lake margins. Once tapping is initiated outflow through the new conduit results in rapid lake drainage. River networks in lowland permafrost are likely inter-twined with thaw lakes because flood discharges from breached lakes may far exceed storm or spring melt discharges in these generally semi-arid regions. However, the effects and magnitude of thaw lake floods remain largely undiscovered.

This thesis examines the following problems: 1. What is the volume of thaw lake floods, and how do these compare to annual spring freshets? 2. What is the frequency of thaw lake drainage events on low order streams? 3. What are the dimensions of channels formed by thaw lake drainage? 4. What is the morphological and sedimentological evidence in low order river channels of thaw lake drainages? To address these questions, I collected measurements from the Running River region, Yukon Coastal Plain, Western Canadian Arctic. I use five methods to investigate these problems including: 1. sedimentological analysis of channel terraces; 2. channel morphology from differential GPS surveys; 3. hydrology of current stream flow rates in a low order stream; 4. calculation of stream power for base flows, spring freshet, and thaw lake flood discharges; 5. bathymetric and volumetric analysis of a drained thaw lake and drainage channel using differential GPS surveys.

The Yukon Arctic Coastal Plain landscape is flat, with pre-existing topography that has been shaped and moulded by thaw lake and river activity. It lies within the zone of continuous permafrost (Rampton 1982). Vegetation at this high latitude is sparse compared to temperate regions, consisting of low-lying tundra shrubs, and sedge grasses, with small willow trees restricted to sheltered river valleys and lake shores.

The Running River is one of four major rivers of the Yukon Coastal Plain draining north to the Beaufort Sea (see Fig. 1.1). Grayling Creek is a low order tributary to the Running River (see Fig. 1.1). This study focuses on measurements of valley morphology and drainage basin of Grayling Creek, and on drained basins within the Running River drainage basin.

Chapter 2: Background to Processes Affecting Arctic Low Land Environments

2.1 Permafrost

Permafrost refers to ground (soil and rock) that remains frozen (< 0 ℃) for at least two years (French 1996). Permafrost is not always defined by water in its solid state because water within earth materials can remain unfrozen below 0 ℃ owing to freezing point depression by the chemical content of dissolved solids. Where mean annual ground temperature is below the freezing point of mineralized ground water, permafrost will form (Williams and Smith 1989). Water in permafrost will freeze and expand by approximately 9% of its original unfrozen volume.

Permafrost exists at depths where seasonal temperature variations are insufficient to heat and thaw the ground. The amount of frost penetration into the ground depends on four primary factors: 1. the mean annual ground temperature must be sufficiently cold for freezing to occur; 2. the degree of the annual temperature cycle at the ground surface meaning how continental the climate is; 3. ground surface conditions, especially whether there is snow cover or not; 4. thermal properties of the soil including heat capacity and thermal conductivity (Williams & Smith 1989). In many periglacial regions permafrost results from extended winter periods of significant cold and relatively short summers. For example, the average temperature between November and April on the Yukon Coastal Plain is approximately -21.0 ℃ (Environment Canada 2004).

The term talik is used to describe unfrozen volumes of soil or rock contained within or above permafrost. Supra permafrost taliks are located at the permafrost table,

closed or intra-permafrost taliks are contained within permafrost, and sub-permafrost taliks occur beneath permafrost (see Fig 2.1). The thin layer of ground near the surface that freezes and thaws annually, is called the active layer (see Fig. 3.1).

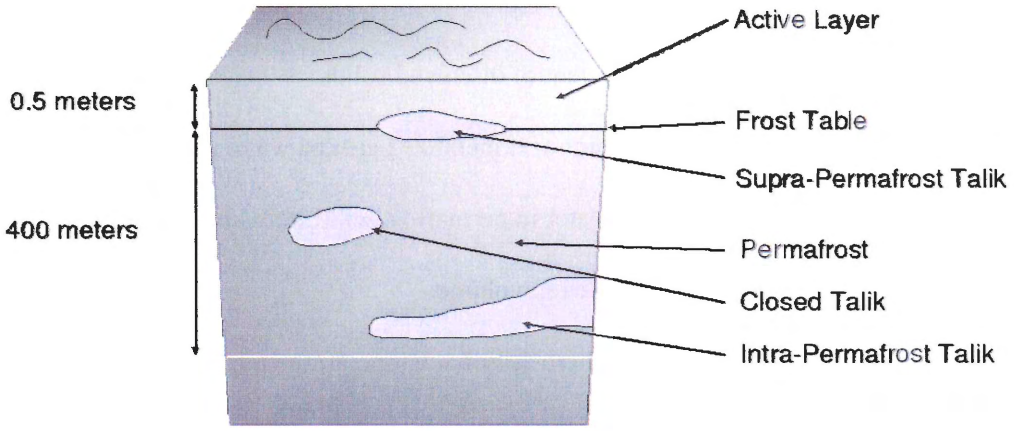

Figure 2.1 A schematic diagram of permafrost, approximate thickness's of active layer and permafrost on the Yukon Coastal Plain (modelled after French 1996).

Permafrost presently occupies roughly one quarter (25%) of Earth's ground surface (see Fig. 2.2 & 2.3). Most permafrost is greater than 1000 years old (Williams and Smith 1989) and is primarily found in alpine environments and high latitude environments (French 1996). High latitude permafrost regions can again be further divided into zones of discontinuous/sporadic and continuous permafrost (French 1996). Discontinuous permafrost has areas of frozen ground separated by areas of unfrozen ground. Frozen ground is present everywhere in continuous permafrost localities except

for isolated thaw zones centred around lakes, river channels, and standing water bodies (French 1996). Distribution of both continuous and discontinuous permafrost is primarily controlled by climatic variations in temperature, precipitation, snow cover in the winter, magnitude and length of cold winters, and the maximum amount of thaw that can take place during the short summer period. Field observations in Canada and Alaska have yielded mean average annual air temperature values for the limit of the continuous permafrost zones from -6 to -8 °C (French 1996).

Permafrost thickness has been measured in Alaska to some 650 meters thickness, and in Canada's Cornwallis Island to a thickness of 400 meters (Linell and Tedrow 1981). The thickest permafrost measured to date was sampled along the Markha river bank in Siberia, where permafrost thickness of 1500 meters has been measured (Linell and Tedrow 1981).

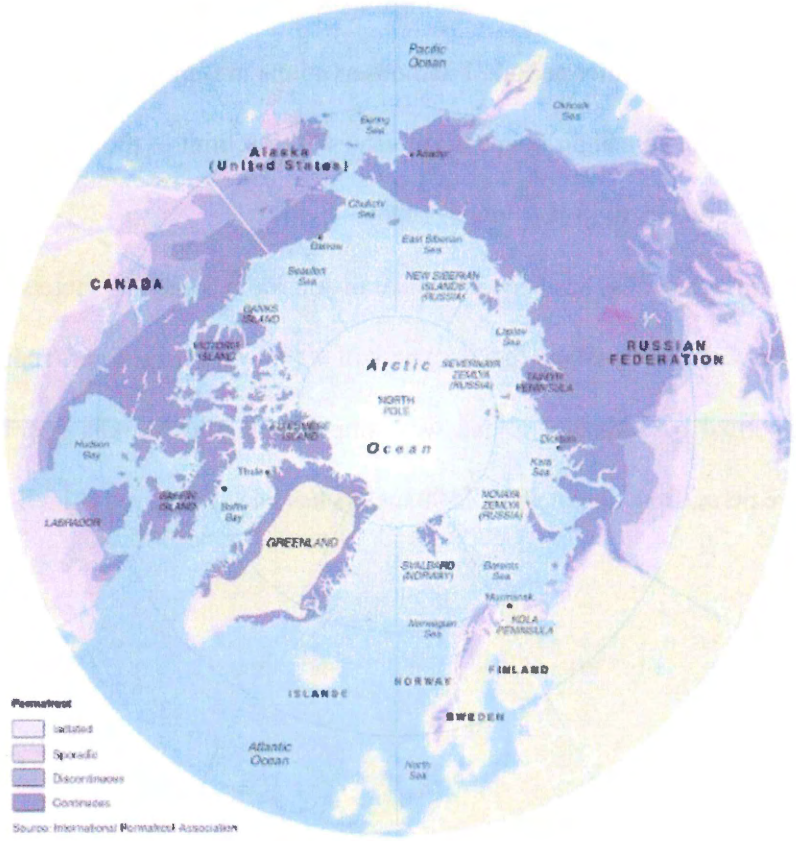

Figure 2.2 Global distribution of permafrost (taken from IPA 2000).

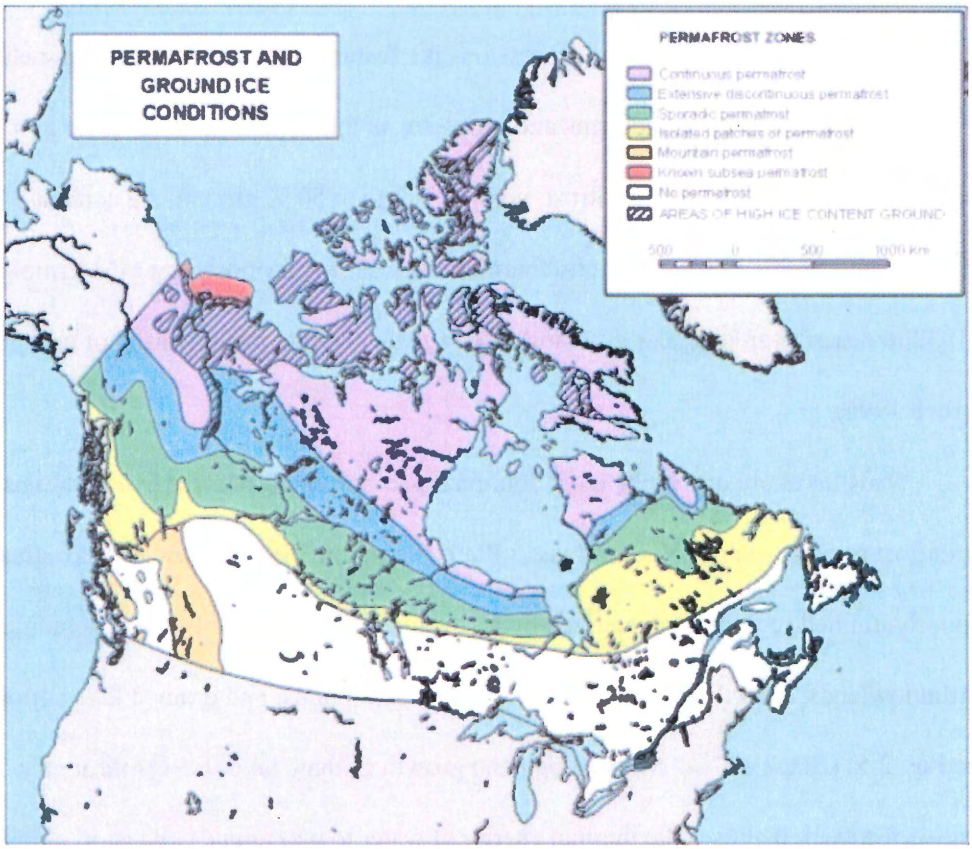

Figure 2.3 Distribution of permafrost types in Canada. The study area is located in continuous ice rich permafrost.

2.2 Thaw Lake and Thermokarst Topography

Thaw lakes are one member of a class of thermokarst landforms which result from thawing and collapse of ice rich permafrost (see Fig. 2.4) (ACGR 1988). The name derives from karsts found in carbonate and evaporitic rocks that form by dissolution processes, except that thermokarst subsidence derives from thermal processes. Besides thaw lakes, thermokarst consists of depression-like features that include alas and melted ice wedges (Ritter 2002). Landforms and processes in themokarst terrains occur as a result of thawing of ice rich permafrost, with greater than 50 % ground ice content (Williams and Smith 1989). The term thermokarst was first proposed by MM Ermolaev in 1932 to describe an irregular hummocky terrane that results from melting of ground ice (French 1996).

Thaw lakes are one of the most dominant geomorphic processes in continuous permafrost regions such as Yukon Coastal Plain (Rampton 1982). Thaw lakes originate in poorly drained regions characterized by low centred ice-wedge polygons, including coastal lowlands, fluvial terraces, outwash plains, loess plains, and drained lake bottoms (see Fig. 2.5) (Black 1976). Morphology and growth of thaw lakes occurs through a positive feedback that uses the thermal energy of water to perpetuate expansion of lake margins (Burn 1992). Expansion of lake margins is achieved when the initial depression, created by collapse and subsidence continues to decay ground ice, allowing continued collapse and subsidence of lake margins to occur (see Fig. 2.6) (Ritter 2002).

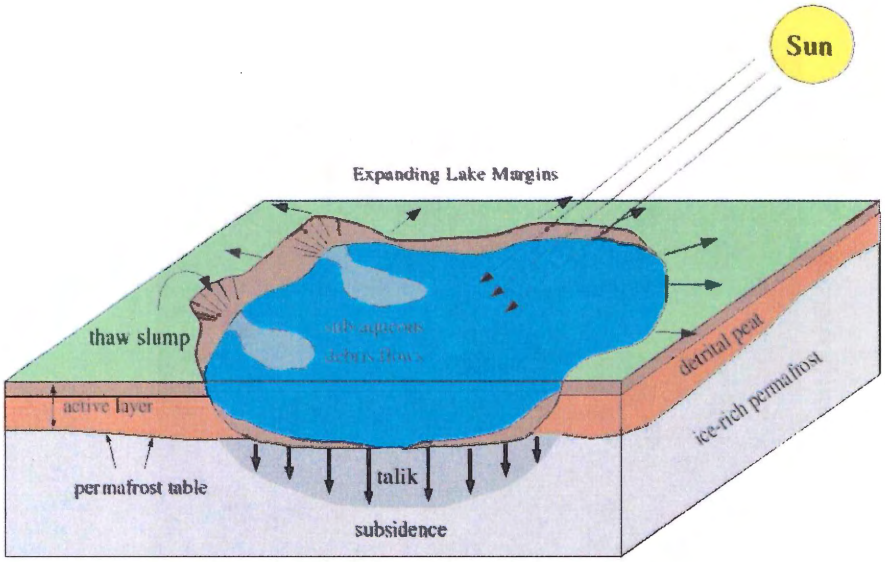

Figure 2.4 Schematic drawing of a thaw lake with expanding margins due to heating and melting of permafrost (modified from McIntosh 2005).

Ablation of ground ice occurs in two ways, first through lateral degradation that allows surface lake water to expose ground ice and secondly through vertical degradation occurring through alteration of surface thermal properties insinuating melting (Ritter 2002). Thaw lake formation occurs best when the thermal equilibrium is disturbed at the surface and an abundance of ice wedges is present. Initiation of melting is primarily induced by a disturbance in the thermal equilibrium of permafrost resulting in an increase in active layer depth (French 1996). Collapse and subsidence therefore can occur as a function of the new active layer equilibrium depth and through super-saturation of degrading permafrost (see Fig. 2.4) (French 1996). Three main factors can induce to thaw lake formation (French 1996, Williams and Smith 1989). Firstly through changes in

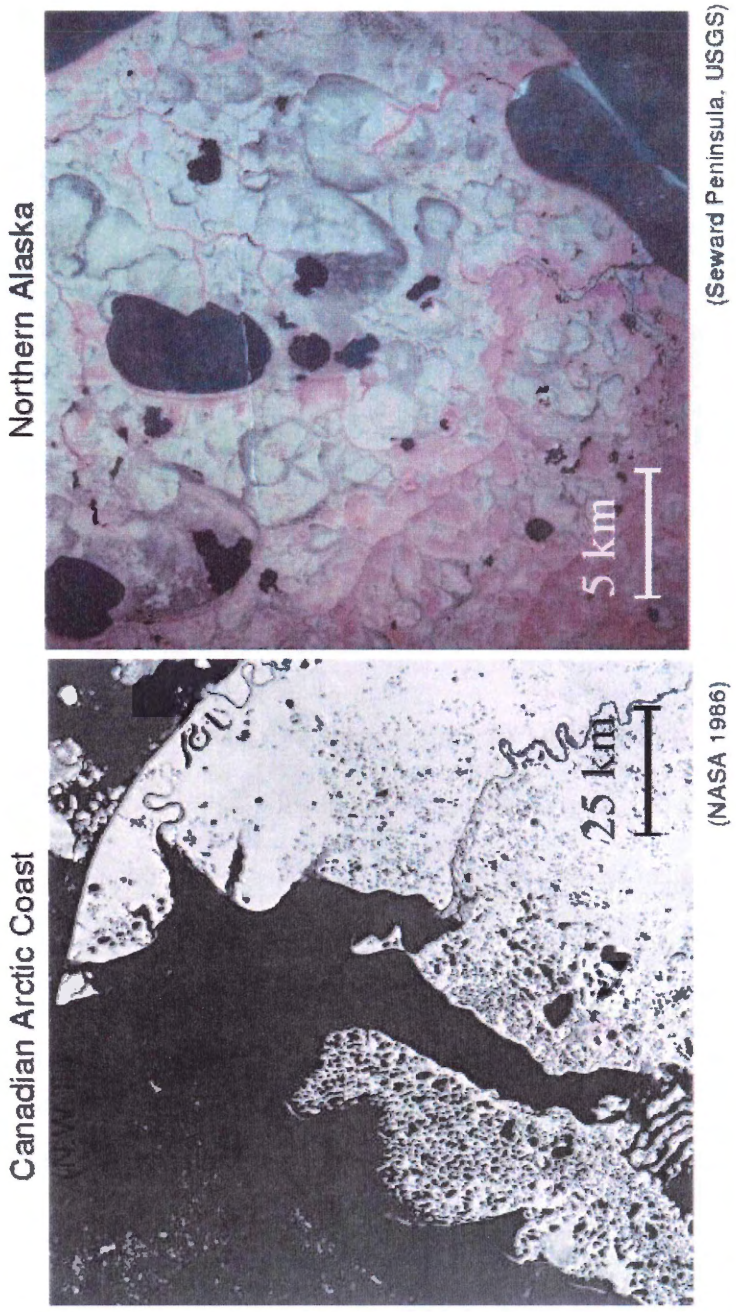

Figure 2.5 Air photos exhibiting thaw lake populations, 10-40 % current and 50-100% relict on Arctic coastal plains.

regional climate, thaw lake development is most intense when there is an associated rise in mean annual ground temperature, and an increase in the amplitude of temperature fluctuations. A combination of these two climatic induced factors can result in a maximum growth in active layer depth. Secondly under stable climate, thermokarst can develop as a result of a variety of geomorphic and/or vegetation disturbances of the ground surface. Changes in conditions can be anthropogenically induced or induced by naturally occurring changes in vegetation and surface processes. Third, the amplitude of

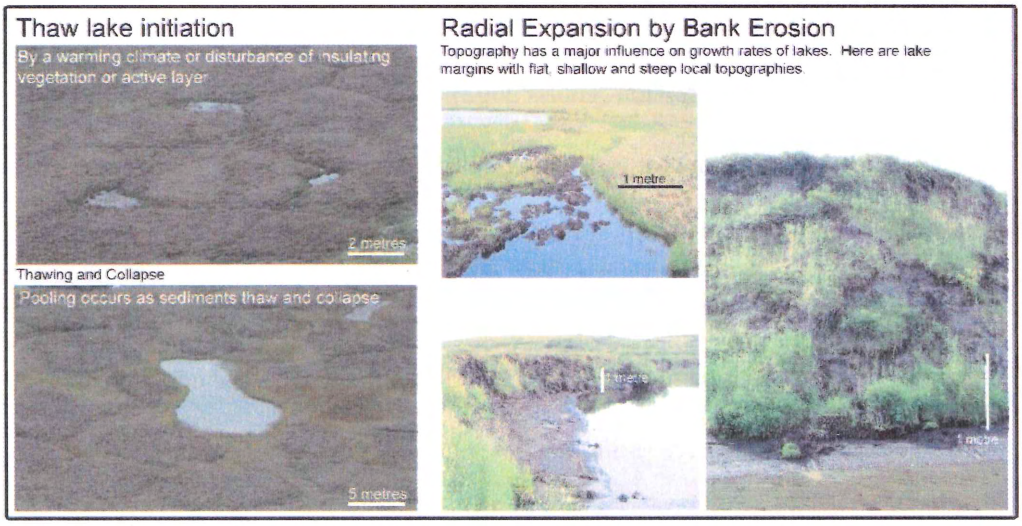

Figure 2.6 Pictures from the Yukon Coastal Plain of thaw lakes and how they initiate, and expand radially, usually expansion commences in an irregular shape, but eventually turns circular to elliptical in shape. Later stage thaw lakes are characterized by having relatively smooth boundaries. (Taken from McIntosh in field 2004).

thermokarst growth is dependent on increases in the magnitude of active layer thickness, ice content in the soil, and the amount of tectonic activity experienced by the region. Ground ice volumes control population, distribution and morphology of thaw lakes. Thermokarsts are most prevalent in tectonically inactive and stable areas like the Yukon

Coastal Plain that will not shift and move allowing lake formation and growth (French 1996, Williams & Smith 1989).

Thaw lakes that occur in lowland periglacial environments are often rounded to semi rounded in shape (French 1996). Thaw lake basins are very shallow relative to diameter; they can grow to 1-10 km across but most are between 300 and 400 meters in width, and most only 3-7 meters deep (French 1996, Williams & Smith 1989). In some cases, coalescence of adjacent polygon pools creates larger pools that can eventually form a lake (French 1996). During coalescence water from one lake basin of higher elevation may overflow into an adjacent lake basin. This process continues until the two eventually meet a stream channel or depression (Harris 2002).

Erosion at thaw lake margins occurs in irregular patterns in early lake stages, but through melting margins and growth lakes assume a regular smooth circular shape (French 1996). Lake water heated by solar radiation undercuts lake margins causing degradation and melting of permafrost. Collapse of sediment and vegetation occurs causing lake margins to advance, enlarging lake area and volume. As thaw lake margins expand, gradual infilling occurs and some hypothesis that infilling is responsible for empty lake basins. This theory is unlikely to be true, because processes of margin melting, collapse and slumping cause thaw lake growth. Catastrophic lake drainage through tapping of topographic lows is a more probable solution to partially and completely drained thaw lake basins. Evidence of thaw lake drainage has been documented on numerous occasions, but has relatively been unstudied. Topographic

lows through which lakes may drain include other thaw lakes, river channels, head-ward erosion of streams along ice wedge networks, and by coastal margins (French 1996). Once drainage is initiated a massive amount of water is released cutting large drainage conduits in a short period of time (1-2 days) (Marsh & Neumann 2001). As a result of rapid drainage and incision, drainage channels may have a box canyon shape (Mackay 1981).

2.3 **Alluvial and Fluvial Processes**

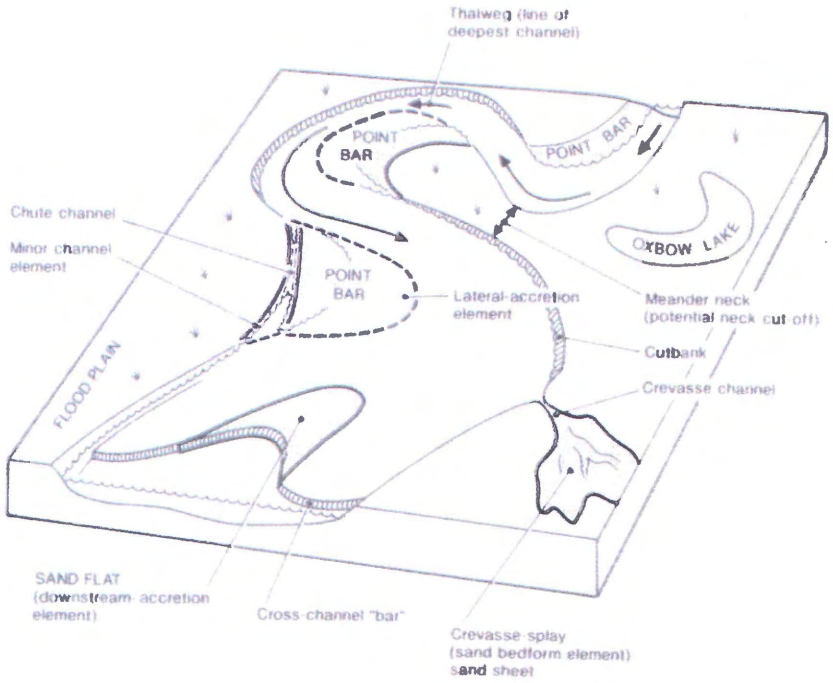

Figure 2.7 Diagram showing the different aspects of a basic river system (Taken from Miall 1992).

Alluvial deposits occur in a wide range of tectonic settings and are sensitive indicators of changes in tectonism and sea level (Miall 1992). Deposits are

characteristically clastic and range in grain size from the finest muds to very coarse boulder conglomerates. There are two major spatial scales of deposition that can be examined, a large scale examining depositional bars and a small scale examining small bedforms and other types of stratification (Miall 1992). Examining larger scale features in rivers has lead to the recognition of four different river channel styles; straight, braided, meandering and anastamosing (see Fig 2.8). Bedforms and bars are created by the transport and deposition of sediment (see Fig. 2.7). Transportation occurs by through traction currents that transport cohesion-less sediment as individual grains, and by through mass transport of sediment by liquefaction on sloping surfaces in sediment gravity flows (Miall 1992). Large grains slide and roll along river beds as bedload and smaller grains are held in suspension for short periods of time as bed contact load, therefore being bounced down the river bed (Miall 1992). Turbidity currents, gravity flows, and debris flows are all examples of how sediment can travel as one massive body. The process of liquefaction resulting from addition of large amounts of water allows sediment on slopes to become unstable and collapse. In both traction currents and sediment gravity flows small grains such as silt and clays are held within the water column for longer periods of time, this results in a natural sorting of sediment grain sizes. Large boulders and cobbles are deposited near the head waters of rivers and grade gradually to silts and muds in deltas, flood plains, flood plain ponds and abandoned channels down stream.

The ability of a river to transport material depends the streams power that is controlled by two factors: competency and capacity. Competency relates to the strength of flow in a river through velocity and shear stress, and indicates the maximum size of sediment a river can transport (Miall 1992). Capacity reflects the magnitude of discharge from a river and is indicated by the total volume of sediment moved by a river (Miall 1992). Competency and capacity are ways of measuring a river's potential to transport a maximum grain size and a maximum volume of sediment.

Entrainment and transport of sediment as bedload is analysed in terms of stream power per unit width of a channel (Leopold *et al.* 1992). Stream power is specific to changes in specific weight of the fluid, discharge, and slope all per unit area of the stream bed, representing a combination of velocity and shear stress (Leopold *et al.* 1992).

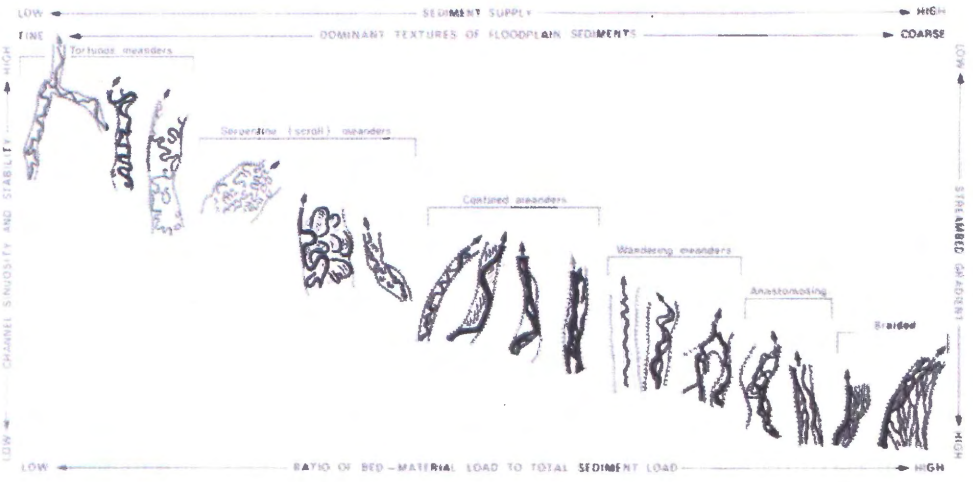

Figure 2.8 Diagram showing how channel morphology changes as aspects like sediment supply, bed load, channel stability, and stream gradient change and the resultant channel style (Taken from Selby 1985).

Arctic rivers and streams flow for only a short period of time each year leading to a general consensus that rivers have little effect in developing and shaping periglacial landscapes (Ashmore & Church 2001). Unlike lower latitude river networks there is little flow in large rivers and no flow at all in low order streams in the winter months. Spatial and temporal variations control and restrict all subsurface water flow to the thin active layer (Williams & Smith 1989). Flow in Arctic streams and rivers is not dominated by rainfall like in lower latitudinal rivers but rather is dominated by the rapid melting of snow and ice experienced each spring in an annual freshet lasting for a week to two weeks.

Groundwater contribution to stream flow is negligible in continuous permafrost regions (Williams & Smith 1989) because it is almost completely restricted to the active layer. Fluvial processes are strongly influenced by the presence of permafrost at depth and by snow and ice covers in the winter months (Woo & Sariol 1981). All large rivers such as the Colville River in Alaska and the Mackenzie River in Canada maintain a base flow in the channel thalweg during winter months (Williams & Smith 1989).

River valleys of the Yukon Coastal Plain contain a number of elements. Valley walls, river terraces, valley plains, and active modern river channels are characteristic elements in river valleys. Valley plains are the lowest terrace, and are also referred to as flood plains (McDonald & Lewis 1973). Small amounts of inundation from modern channels allow observations to be made of flood deposits in the sedimentary record recording past flood events. Flood couplets are fining upwards sequences represented by

two definitive units -- a coarse bed overlain by a fine bed. The coarse bed represents the flooding event experienced on the flood plain, and the fine bed represents a slack water deposit as flow rates slow. River terraces are created by episodic alluvation and entrenchment, as river channels incise downwards into valley plains (see Fig. 2.9) resulting in the formation of terraces representing past flood plains. Terraces can be paired or unpaired depending at what point in the channel the observation took place. River stability is a determining factor in terrace formation and as to whether terraces are paired or unpaired. Steep terrace faces are unstable and prone to mass movements as river channels incise downwards (McDonald & Lewis 1973). Valley walls extend upwards from the most elevated terrace to the upland surface (McDonald & Lewis 1973). Valley walls also are characteristically steep and often unstable resulting in mass movements of sediment. Steep, narrow valleys with few or no terraces are characteristic of rapid incision rates whereas wide, shallow valleys are characteristic of slower rates of incision.

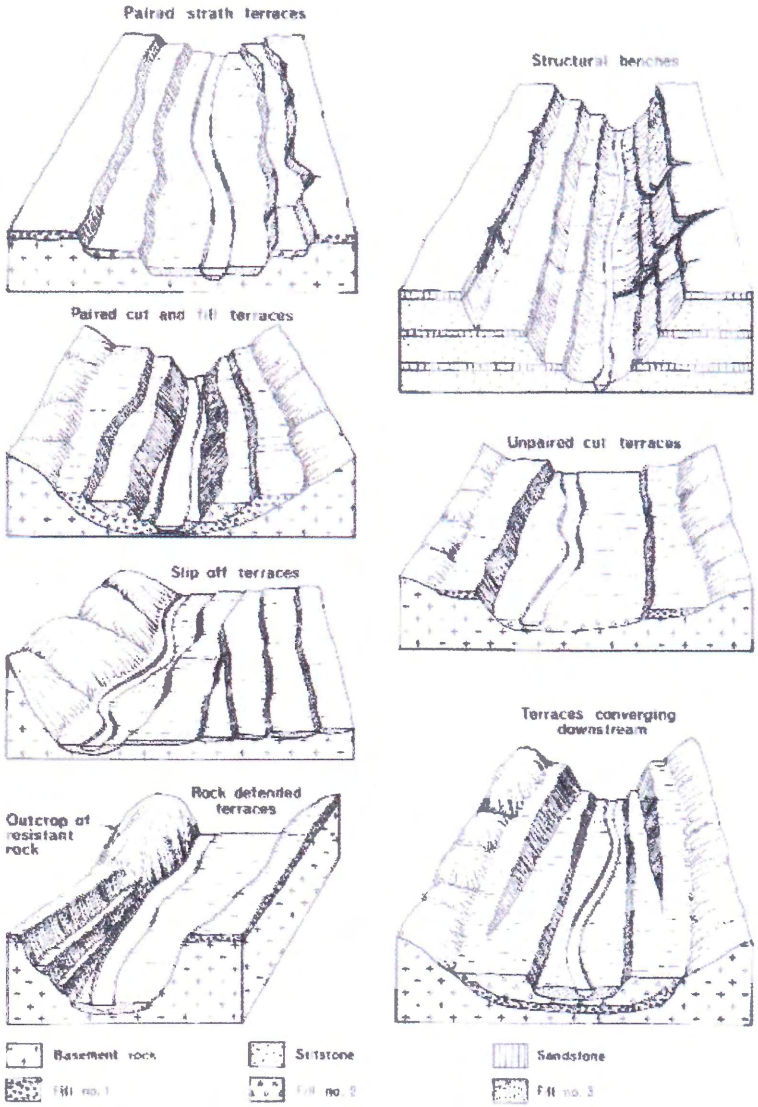

Figure 2.9 Diagram illustrating the various styles of terraces (Taken from Selby 1985).

Chapter 3: Geologic and Climatic History of the Yukon Coastal Plain

3.1 Geologic History

In this chapter I briefly describe the bedrock, Quaternary geology, climate, and glacial events that have affected the Yukon Coastal Plain. The Barn Mountain range also is discussed due to its importance in the Running River's drainage basin. The Yukon Coastal Plain commonly is divided into two physiographic regions, mountain proximal and coast proximal (Rampton 1982). However in this chapter the geologic background of the coastal plain is described as one unit.

3.1.1 Pre Quaternary Geology

This section discusses the Pre-Quaternary geology of the Yukon Coastal Plain and the Barn Mountains, the origin of the Running River. The emphasis on bed rock geology illustrates that the Yukon Coastal Plain has been tectonically inactive since the late Tertiary.

The Barn Mountains today are a representation of the Barn uplift that occurred during the Cordillerian Orogeny (Dyke 1996) and the easternmost section of the Romanzof uplift which created the British Mountains. The Barn uplift is bounded between the Old Crow Plateau and the dextral Barn fault (Norris 1996), and is a horizontally shortened tilt block (Dyke 1996). It is characterized by a northerly elongate area of highly compressed lower Paleozoic strata that is a continuation of the Road River Formation of the Richardson Mountains (Norris 1996). The tilt block is bound by sub-vertical, north-trending faults that have curviplanar to listric geometry (Norris 1996).

Lithologies exposed in the uplift include Devonian aged porphyritic granite found on Mount Fitton; chert, conglomerate quartzite, shale, coal and limestone of the Carboniferous Kekiktuk and Kyak Formations; limestone of the Triassic Shublick Formation; shale of the Jurassic Kingak Formation and Cretaceous shales and sandstones (Rampton 1982). The Yukon Coastal Plain is a paleo-plain constructed through erosional and depositional events associated with the transgressions and regressions of the Beaufort Sea (Rampton 1982). Onshore portions of the Beaufort Shelf are underlain by shales and sandstones deposited during the Jurassic and Lower Cretaceous periods (Rampton 1982). Around the region of the Running River, Upper Cretaceous conglomerates, sandstones, shales, and mudstones underlie Tertiary aged conglomerates, sandstones, shales, and coal layers (Rampton 1982).

The Late Cretaceous and Tertiary are segmented into two distinct phases of sedimentation (see Fig. 3.1): an early sedimentary phase lasting from the Cenomanian to the Maastrichian that deposited cratonic sediments, and a late phase of sedimentation that started in the Maastrichian and still continues today (Dixon 1996).

The early phase is characterized by coarse clastic sediments that were deposited in shallow foreland basins. Creation of foreland basins in the northern Yukon occurred as part of the Cordilleran Orogeny that affected most of western North America. Sediment

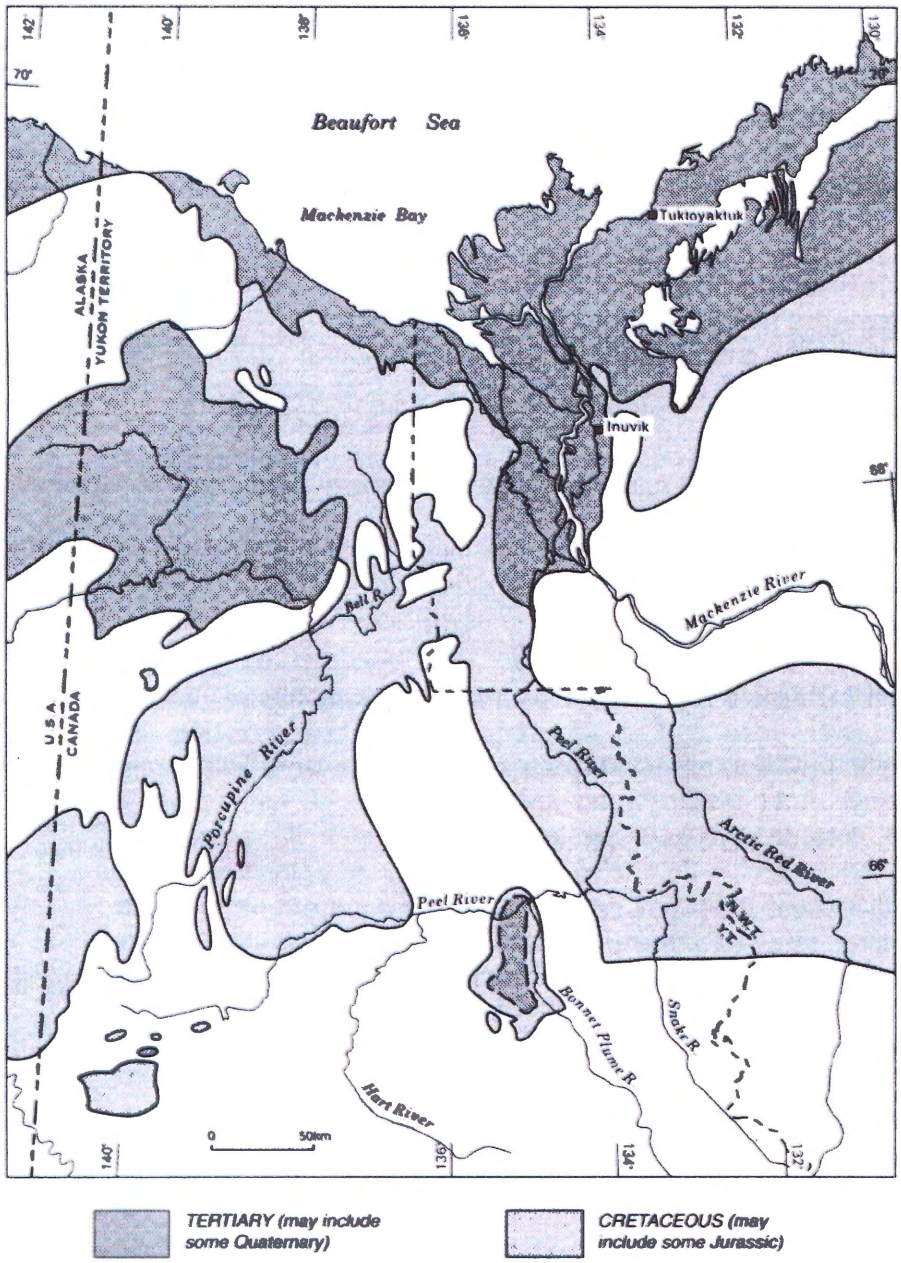

Figure 3.1 Tertiary and Cretaceous strata locations Yukon Coastal Plain (Dixon 1996).

size decreases progressively northward in the Northern Yukon, eventually fining to shale near the Beaufort Sea. Strata of the Yukon Coastal Plain consists of an organic rich outer shelf to basinal facies (Dixon 1996). During this early period of sedimentation two major transgressive events occurred separated by an unconformity (Dixon 1996). The first took place between the Cenomanian and Turonian in the Late Cretaceous and the second occurring between the Santonian and Campanian during the Late Cretaceous.

During the Maastrichian a shift from a locus of cratonic sedimentation occurred. This signified the commencement of late phase sedimentation, where the northern continental margin became the main depositional centre for sediments (Dixon 1996). During late stage sedimentation, large scale deltas and delta complexes were formed. Deltas that formed in early parts of the Tertiary are concentrated on the western end of the Beaufort shelf, while later stages of formation during the Pliocene migrated to more easterly localities (Dixon 1996).

3.1.2 Quaternary Geology

The Quaternary geology is sub-divided into three sections based on the glacial history of the Yukon Coastal Plain, termed pre-glacial, glacial, and post-glacial. More than one glacial event occupied the Yukon Coastal Plain, but only one glacial period formed and deposited the present landforms (Rampton 1982). The event was the Buckland Glaciation which occurred roughly from 130 ky to 75 ky years ago, equivalent to Oxygen Isotope Stage (OIS) 6. Any deposition after Buckland Glaciation is termed post-glacial, and any deposition previous to the Buckland Glaciation is termed pre-glacial

(Rampton 1982).

Prior to the Buckland Glaciation, sedimentation and erosion took place under varying climatic conditions. The most obvious and dominating features deposited during the Quaternary occurred prior to the Buckland glacial event, and consist of alluvial fans, associated deposits to alluvial systems, and antiplanation terraces associated with higher elevations in the mountains adjacent to the Yukon Coastal Plain (Rampton 1982). Alluvial and terrace deposits are characterized by thick beds of gravels that are inter-bedded with finer grained sands (for Quaternary deposits see Appendix A). Conditions during deposition fluctuated between temperatures satisfactory for ice wedge growth and temperatures satisfactory for ice wedge degradation. Climate warming after cold periods either partially degraded or completely degraded ice wedges that formed during the previous cold period, depending on the degree of warming (Rampton 1982). Occasionally ice wedges were preserved leaving a cast of their former shape. Inter-bedded into sand and gravel layers are smaller inter-beds of silt, woody fragments and organic detritus from plant and biological matter.

Alluvation continued throughout the Quaternary until the advance of Buckland ice sheets. Some till like material (diamictite) overlie pre-Buckland alluvial and terrace deposits, is believed to be part of a pre-Buckland aged sequence that probably only affected the south-eastern most section of the Yukon Coastal Plain (Rampton 1982). Overlying the diamictite are flood plain or deltaic deposits (Rampton 1982).

The Buckland glacier covered the Yukon Coastal Plain and adjacent Mountains depositing the majority of landforms present today. There is no evidence of another glacial event having affected the Yukon Coastal Plain since the Buckland event of OIS 6 age. There is evidence of possible OIS 2 (10000 to 25000 years ago) ice sheets having affected the edges of the Yukon Coastal Plain and the Richardson Mountains (Rampton 1982). The Buckland sequence is defined as being the glacial event that extended past the limits of the later OIS 2 glaciation. During the retreat of Buckland ice sheets a possible stand still or re-advance occurred, called the Sabine Phase, that is inferred by the presence of a long morainic ridge with associated outwash channels and gullies (Rampton 1982). Glacial limits can be traced and followed from the Richardson Mountains in a North-Westerly direction along the Barn Mountains and Buckland Hills to the Malcolm River. The maximum extent of glaciation is truncated by the Beaufort Sea coast between the alluvial plains of the Firth and Malcolm Rivers. Topographical features representing the terminal limit of glaciation include morainic ridges, kame terraces and fans, eskers, melt water channels, glacial lakes, and the maximum elevation of ice is shown by erratics dropped during glacier retreat (Rampton 1982).

Present day moraines only vaguely resemble moraines originally deposited by glaciers, as thermokarst alteration is accountable for the morphology of the many rolling and hummocky morainal deposits. Accompanying Buckland glacial sediments also are complex sequences of lacustrine deposits, organic silts, and many layers of humified and fibric peat that are closely related to thermokarst activity and evolution.

Commencement of thermokarst growth and evolution is due to climatic changes that occurred long after the retreat and deglaciation of the Buckland phase (Rampton 1982). All deposits and alterations that occurred after the retreat of Buckland glacial ice are termed to be post-glacial, however there is some evidence of Laurentide ice sheet presence on the most south-eastern fringe of the Yukon Coastal Plain. Generally post-glacial deposits are of a non-glacial origin and consist of related phenomena to ground ice, thermokarsts or thaw lakes, solifluction lobes, and fluvial landforms and deposits.

Partially entrenched and confined rivers are common on the Yukon Coastal Plain, most of which are gravel bedded and have meandering, braided and wandering channel patterns (see Fig. 2.8). The majority of river channels on the Yukon Coastal Plain have coarse, clastic boundaries, and characteristically have a high width to depth ratio (McDonald & Lewis 1973). Primary modes of sediment transport are as bedload. Channel beds are armoured by selective transport of fine sediment, and imbrication of sediment grains (McDonald & Lewis 1973).

3.2 Climate

The Yukon Coastal Plain has a harsh, cold, climate considered to be an Arctic desert, in which arid to sub arid climatic conditions persist year round. Winter months are predominantly affected by cold continental air flowing off the continent northward to the Beaufort Sea. Sub-zero mean temperatures occur approximately 250 days per year (Rampton 1982, Environment Canada 2004). Temperatures experienced on the Yukon Coastal Plain reach an average maximum monthly of 10.0 ℃ in July and a minimum of

-25.0 ℃ in February. Mean annual surface temperature is -10.0 ℃ (see Fig 3.2). Summer months on the coastal plain are affected by warmer maritime air flowing from the sea landward onto the coastal plain.

The Yukon Coastal Plain receives little precipitation annually (see Fig 3.3) and is considered to be a polar desert (Rampton 1982). August is the rainiest month receiving roughly 53.0 mm of rain and on average 4 cm of snow. October is the snowiest month where roughly 30.0 cm of snow falls on average. Snow persists for the duration of the winter (see Fig. 3.4) reaching a mean maximum depth of approximately 36.0 cm in April. Precipitation annually occurs as 50 % snow and 50% rain, and an average of 50 cm of snow falls annually (Environment Canada 2004). Fog and cloud cover are fairly rare in winter due to sea ward direction of the wind, however in summer greater amounts of fog and cloud occur in coastal areas. Greater amounts of precipitation occur south of the Yukon Coastal Plain in the mountains, and drainage basins transport water from the mountains and coastal plain northward to the Beaufort Sea.

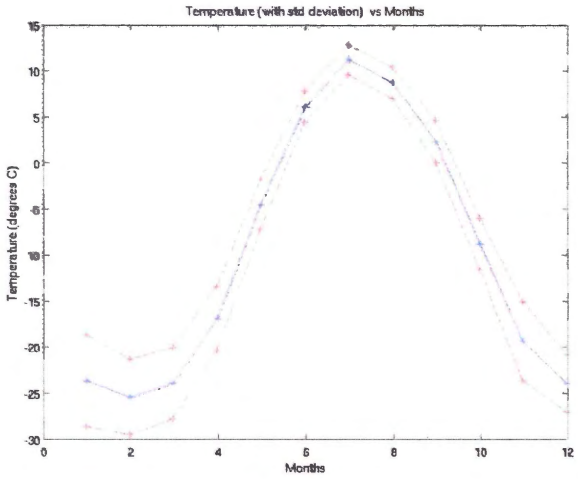

Figure 3.2 Mean temperature through the year on the Yukon Coastal Plain. Red lines show standard deviation over the 50 year period of record (calculated from raw data provided by Environment Canada 2004).

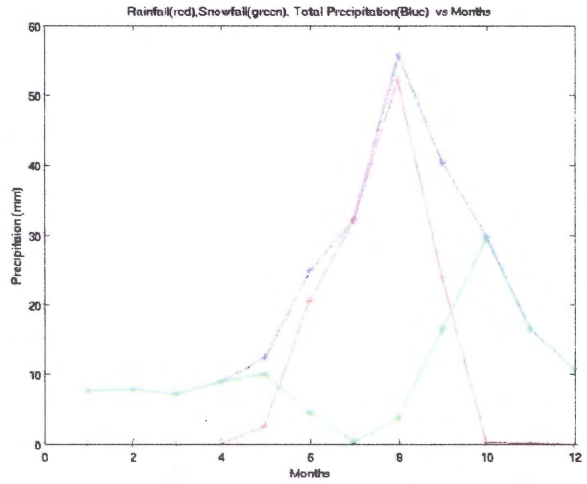

Figure 3.3 Mean precipitation of each month throughout the year (calculated from raw data provided by Environment Canada 2004). Red is monthly rain fall, green is monthly snow fall, and blue is the total monthly precipitation.

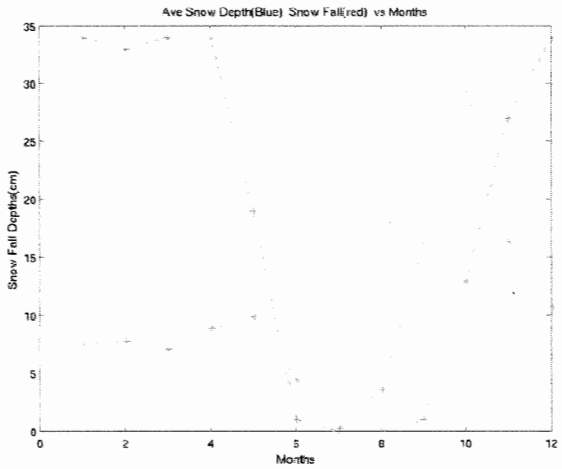

Figure 3.4 Mean snow depths and the snow deposited in each month experienced on the Yukon Coastal Plain (calculated from raw data provided by Environment Canada 2004). Red represents the average snow depth and blue represents snow fall in that month.

3.3 Permafrost

The Yukon Coastal Plain is part of the continuous permafrost zone, in which frozen ground is continuous beneath the seasonally frozen and thawed active layer. Ground temperatures found at the mouth of the Babbage River, north of the Running River are -8.5 +/- 1.5 ℃, and ground temperatures at the northern end of the Mackenzie Delta, south of the Running River are -2.5 +/- 1.5 ℃ (Rampton 1982). The permafrost layer extends to depths between 400 to 500 meters thickness beneath the Yukon Coastal Plain (Rampton 1982). Thickness decreases beneath bodies of water, both standing (lakes and ponds) and flowing (rivers and streams). Zones of unfrozen material known as taliks exist beneath major streams, flood plains, drained and full lake basins, spits, bay mouth bars, and any other place that experiences a negative flux of mean ground temperature

(Rampton 1982). Active layer thickness varies between 0.5 and 0.3 meters. High percentages of ground ice in excess of 50 % occur in the permafrost throughout the Yukon Coastal Plain (Rampton 1982).

3.4 Vegetation

The Yukon Coastal Plain is covered by tundra type vegetation consisting of low lying shrubs and grasses < 2 -3 meters high. Sedge (*Carex*) species dominate but some variability arises from local slope and drainage conditions (Rampton 1982). Well drained slopes are characterized by cotton grass (*Eriophorum vaginatum)* and sedge (*Carex)* species of vegetation (Rampton 1982), which prefer elevated dryer surfaces opposed to flat lying areas dominated by wet sedge (*Carex aquatilus*) meadows (L. Plug, Personal Communication 2004). Sheltered stream valleys and lake shores are refuges where the tallest vegetation occur, including Arctic willow shrub (*Salix alaxensis*), *Betlanana L.* and *B. glandulosa.*

Chapter 4: Methods and Equipment

Data acquisition conducted in the field occurred in August of 2004 in the Running River area, primarily focusing on Grayling Creek and Bigwok Basin (see Fig. 5.1). Data analysis was conducted at Dalhousie University, Halifax, Nova Scotia. This study is focusing on the affects that thaw lake drainage events have on low order Arctic river morphology.

4.1 Data Acquisition

4.1.1 Grayling Creek and Running River Sedimentary Sections

Between August 18th and 24th 2004, six sedimentary sections (~0.5-2.0 m high, 2.0 m length) were excavated into flood plain deposits of Grayling Creek and the Running River using a 1954 Korean War entrenching tool. Sections GC-1, GC-2, and GC-3 were in the lowermost terraces of upper Grayling Creek approximately 3 km from its exit into the Running River, and section GFP was in the flood plain of Grayling Creek at its mouth (see Fig. 5.1). Two sedimentary sections, RR-1 and RR-2, were excavated into the Running River's flood plain (see Fig. 5.1). Flood plain deposits were described and sampled for each section.

4.1.2 GPS surveys of Bigwok Basin and Grayling Creek:

GPS Surveys

From August 19th to 24th ground surveys of Grayling Creek, and Bigwok Basin were measured using a dual frequency differential Leica GX1230 Global Positioning System (GPS) and a Leica GS20 GPS. Valley cross-sections for approximately 7200 m

of Grayling Creek were measured to obtain accurate valley morphology. Paleo-shores of Bigwok Basin were surveyed and tied together with transects from current lake levels through paleo-shorelines to obtain accurate bathymetric measurements of Bigwok Basin. GPS measurement accuracy is dependent on the initial set up of the system, primarily the height of the carrier conducting the survey, and upon various external factors such as number of available satellites, observation time, ephemeris accuracy, ionospheric conditions, and multipath from satellites. The GX 1230 rover receiver is carried in a backpack, with antenna height measured for each individual surveyor. The GS20 is a hand held receiver held at approximately 1.25 meters above ground level during surveys. Resolution of phase ambiguities can be completed in real time in the field with the GX1230, resulting in instantaneous sub-centimetre theoretical accuracy. However, during our field study the radio link between rover and reference station was inoperative. Measurements were post-processed later in Leica GeoOffice to resolve phase ambiguities; this posed an inconvenience but had no effect on the results.

GPS Systems Technical Data

The System 1230 consists of a dual frequency differential fixed GPS reference station that operates throughout a survey, while the surveyor records moving position data with a second back-pack mounted GX 1230 receiver (the "rover"). The system uses dual frequency (L1 and L2 channel phase) signal from satellites to calculate position, in contrast to most GPS receivers (e.g. recreational hand-helds) which use code data only. Accuracy using differential phase in post processing for normal base lines is 5 mm + 0.5

ppm horizontally and 10 mm +0.5 ppm vertically for static measurements and 10 mm + 1ppm horizontally and 20 mm +1 ppm vertically using kinematic methods. In practice, because our system was back-mounted, we estimate three dimensional position accuracy to be approximately 30 cm, a value supported by tests in which the same line was surveyed with backpack and pole-mounted receivers (Plug, Personal Communication 2005).

The GS20 is a single frequency (L1 channel) receiver. Accuracy using differential phase for static, and rapid static operations is 10mm + 2ppm, and for kinematic operations is 20 mm +2 ppm. Accuracy using differential code when post processing is 30 cm for static and kinematic measurements, and for real time operations accuracy is 40 cm for static and kinematic operations. Because of variability in hand-held height of the GS20, we estimate a three dimensional position accuracy of approximately 1.0 m.

4.2 Data Analysis

Raw GPS data was post processed in Leica GeoOffice and exported as ascii text to MATLAB for visualization and analysis. Distances in meters are plotted three-dimensionally to produce accurate transects across Grayling Creek and the bathymetry of Bigwok Basin. Plots once correlated reveal channel morphology and basin volumes. Rivertools (version 3.0) (RIVEX 2004) was used to calculate the drainage basin area of Grayling Creek from 90 m digital elevation maps (map # 117 A,C, and D) provided by GeoBase (2004).

4.3 Discharge and Flow Rate Calculations

Two localities on Grayling Creek were measured for flow rates and modern channel cross sectional areas. GPS surveys using the Leica GX 1230 were conducted to generate accurate cross sections. Measurements were conducted on straight portions of the channel to allow maximum homogeneity in flow through the cross sectional area. Channel slope through the measured cross sections also was calculated from GPS measurements. Discharge, q, through channel of area a is

$$q = va \tag{1}$$

I used two independent methods to estimate mean stream velocity, v. In the first method I directly measured current velocity (Matchstick analysis) along a short reach of channel. In the second method, I calculated velocity from channel slope, hydraulic radius and channel roughness using the Manning Equation.

Appendix C indicates the time measurements recorded at Flow 1 and Flow 2 on Grayling Creek and the resulting velocities with each corresponding time. The Manning roughness coefficient is between 0.036 and 0.038 for a stream containing cobble sized grains, therefore a Manning value of 0.037 is used (Fetter 2001). The Manning equation for average velocity in an open water channel is

$$V_{ave} = R^{2/3} S^{1/2} n^{-1} \tag{2}$$

where R equals the ratio of the cross-sectional area divided by the wetted perimeter, S is the slope of the channel, and n is the Manning roughness coefficient. Total discharge for drainage of Bigwok Basin and spring freshet from Grayling Creek are estimated by

$$Q = V/(t_f - t_0) \quad (3)$$

where V is the volume of water, and t_f - t_0 is the duration of drainage. Multiple times are used to calculate discharge to provide an appropriate range of discharge values from Bigwok Basin. A time of 30 days is used for Grayling Creek's freshet discharge values (Environment Canada 2004). Stream power, ω, is calculated using

$$\omega = \gamma_w * QS/w \quad (4)$$

where γ_w is the specific gravity of water, Q is discharge, S is stream gradient, and w is channel width. Stream power generates a value for the amount of material a flow can entrain and remove (Leopold *et al.* 1992).

Measurements

Flow 1 measurements were conducted on 2.0 m of straight channel at the two sites on Grayling Creek. The first site, Flow 1, was a rocky channel bed composed of cobble sized grains and with steep banks that are covered by grass and willow trees. The site at Flow 2 was similar to Flow 1, but vegetation entered the water at either side of the creeks banks and the cobbles in the riverbed are slightly larger that at Grayling Creek Flow 1. The two sites are approximately 200 meters apart.

4.4 Radio Carbon Dating

All sedimentary sections were sampled and sediments immediately placed and stored in zip lock bags. Roughly 70 to 150 grams of material was taken for each sample depending on the amount of material available. Samples were transported from the study site to Dalhousie University, Halifax, Nova Scotia in sealed zip lock bags. Upon arrival samples were stored in a refrigerator from September 2004 until December 2004. In December 2004 samples were prepared and sent to Beta Analytic Radio Carbon Dating to be dated. Only one sample was sent away to be dated, 04GCCHF, from unit H section GC-3 (an organic-rich slack water deposit). From sample 04GCCHF we extracted twigs and obvious large organic matter for bulk radiometric dating. The sample was wrapped in tinfoil and placed in a zip lock bag that was labelled with the sample identification number. AMS (Accelerator Mass Spectrometry) was used to produce an accuracy of +/- 0.5 to 3 % of the sample age. AMS dating requires much less carbon (0.00025 - 0.3 g of carbon) than the conventional bulk radiometric dating method, and has a similar accuracy to bulk dating when the sample is younger than 10 000 years old. However AMS dating is more accurate when the sample's age is greater than 10 000 years old. Bulk dating was also not done because of the risk of young carbon contamination from leaching, roots, modern soil, and soil carbonates. Radio carbon dating was conducted by Beta Analytic Radio Carbon Dating, Miami, Florida in December 2004 and January 2005 to show that the deposits in Grayling Creek are indeed post glacial, and also to help determine if Grayling Creek is a glacial outwash channel from the Last Glacial Maximum.

Calibrations were calculated using the most recent database. Multiple probability ranges appear in some cases because of short term variations in atmospheric 14C contents at certain time periods.

4.5 Seasonal Snow Thaw Calculations

Climate data has been collected by Environment Canada since 1957 at Shingle Point, Yukon Canada. Spring snow depths combined with Rivertools calculate the average annual freshet and maximum freshet volume experienced in Grayling Creeks drainage basin. This data when calculated generates discharge and stream power values that are compared to the thaw lake flood volumes, discharges, and stream power from Bigwok Basin.

Chapter 5: Results and Discussion

5.1 Results

5.1.1 Grayling Creek Sedimentary Results

Six sedimentary sections were excavated into the valley floor of Grayling Creek and the Running River adjacent to the modern channel. Three sections in Grayling Creek, GC-1, GC-2, and GC-3, one sedimentary section in Grayling Creeks flood plain GFP, and two sedimentary sections in the Running River, RR-1 and RR-2 (see Fig. 5.1). All sedimentary units analysed are described from top to bottom.

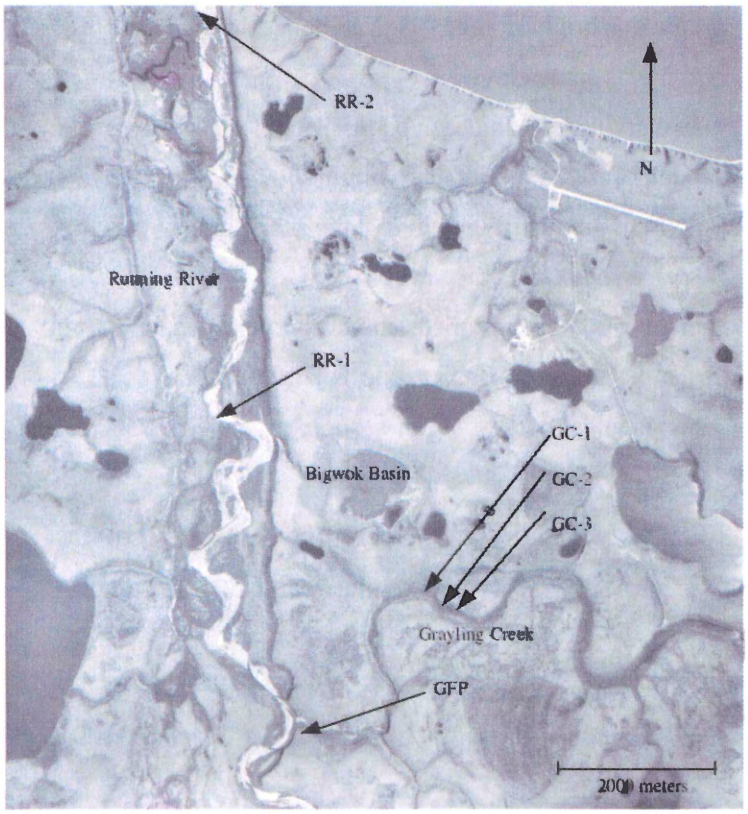

Figure 5.1 Air photo (NAPL 1985) of study area and locations of six sedimentary excavation sites.

GC-1:

GC-1 is located on the southern bank of Grayling Creek and consists of three pits excavated into the river bank one on top of the other, totalling 200cm depth.

Unit (cm)	***Description of Section GC-1***
A. 5-10	-Modern vegetation mat: ledum, dwarf fire weed -coarse sand, pebbles and cobbles (poorly mixed) -no sign of imbrication -abundant modern roots -light brown oxidation of sediment
B. 10-110	-poorly sorted mixture of coarse sand, pebbles up to cobbles -sand and pebble fraction is the largest -contains bright orange oxidized balls, fine sand to silt sized -contains some clays -fine grained organic rich bands 1-5 cm thick -nodules 5-20 cm diameter, bright orange, fine grained sediment -nodules are distributed in organic rich bands
C. 110-135	-coarse sand to pebbles, well sorted -distinct contact with beds above and below
D. 135-200	-pebbles to small cobbles, poorly sorted -this is in the bottom of our section

GC-2:

GC-2 is excavated into the southern bank of Grayling Creek in the lower most terrace, and is approximately 200 cm long and 50 cm high (see Fig. 5.2).

Figure 5. 2 Sedimentary section GC-2 located in Grayling Creek valley, illustrates flood deposits.

Unit (cm)	*Description of Section GC-2*
A. 0-12	-modern soil and vegetation cover -thin cover (0-2 cm) of mosses and grasses -(4-6 cm) modern dark grey organic rich soils
B. 12-23	-fining upwards of fine sand to silt with abundant modern dead root fragments -lenses of dark, finer grained material (1-5 cm thick) in this unit, it is unclear whether these are discrete units (flood soil deposits) or if they are layering within bed

Unit (cm)	*Description of Section GC-2*
C. 23-26	-pebbles to coarse sand, clean hummocky contact below, grading upwards into overlying bed -possible flood deposit
D. 26-36	-fine grained silt to sand with good clean upper and lower contacts -pre flood deposit
E. 36-50	-alluvial gravels with pebbles to the rare cobble -grains are flat lying

GC-3:

GC-3 was excavated into the northern bank of Grayling Creek in the lower most terrace and is approximately 250 cm long and 45 cm high (measured from modern stream level).

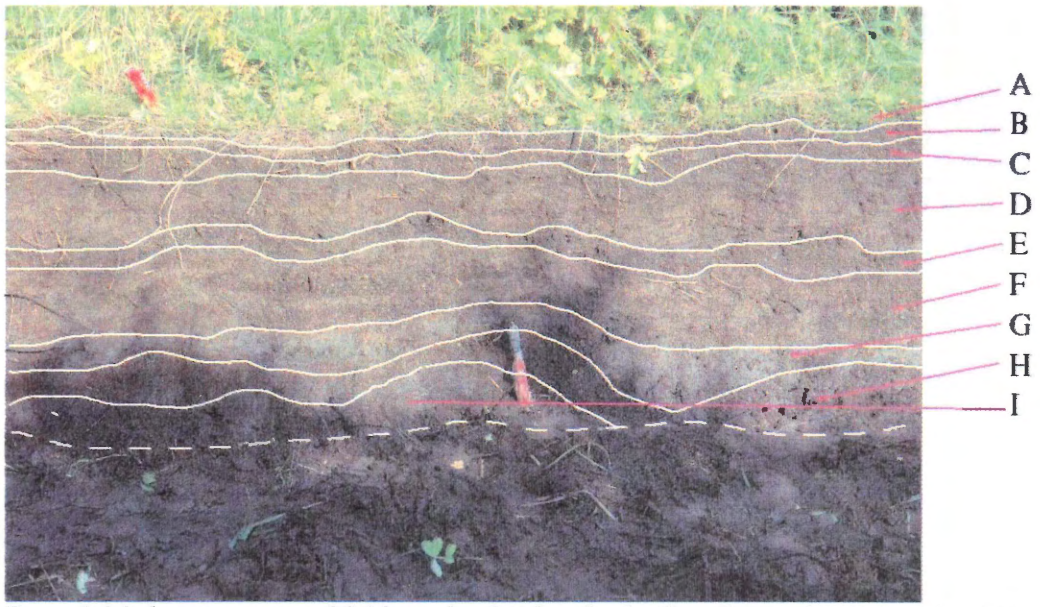

Figure 5. 3 Sedimentary section GC-3 located in Grayling Creek valley, illustrated multiple and variable thickness's of flood deposits in Grayling Creek.

Unit (cm)	*Description of Section GC-3*
A. 0-2	-modern vegetation mat
	-grasses, willows, mosses, shrubs are back from the bank ~100 cm
	-appears to be frequently disturbed by floods (leak and twig fragments caught in willow root grounds)
B. 2-6	-coarse peat mat
	-fine grained sand to silt are plentiful throughout peat fragments
	-modern roots are throughout the unit
C. 6-10	-coarse sand with root fragments
	-poorly sorted, no evidence of fining upwards sequence
D. 10-17	-fine gained sands to silt (silty sand)
	-wavy contacts above and below unit, lower contact is sharp, upper contact is unclear
E. 17-21	-coarse sand to pea-gravel
	-unit pinches and swells, with sharp contacts both above and below unit
	-infrequent pebbles (~2 cm)
	-1-4 cm long detrital wood fragments are present but are infrequent (orientated horizontally), interpret these as slack water deposited detritus
F. 21-30	-multiple (3-5) coarse/fine couplets
	-each bed ~0.5-1.5 cm thick with oxidation between each couplet
	-interpreted as being fining upwards sequences from multiple flood events
G. 30-35	-fining upwards sequence
	-fine unit 1-2 cm thick silty sand, coarse unit 1-3 cm thick coarse sand
	-both fine and coarse layers contain detrital wood fragments orientated horizontally
	-interpreted as being a large flood deposit

Unit (cm)	*Description of Section GC-3*
H. 35-45	-large fining upwards unit
	-fine unit ~5 cm thick clayey silt with fine root fragments that are now dead but thought to have been deposited in situ (Radio Carbon Dated)
	-upper and lower contacts of fine unit are very clear and sharp
	-coarse unit ~5 cm thick coarse to very coarse sand with pockets of pebbles (0.5-1.5 cm diameter)
	-coarse layer has been oxidized
	-interpreted as being large fining upwards flood couplet
I. 45<	-depth of unit is undetermined due to unit entering ground below section
	-silty sand with abundant fine roots, sediment is gleyed (opposite of oxidized)

RR-1:

RR-1 was excavated into the western bank of the Running River into the lower most terrace, between the drainage channel from Bigwok Basin and the Beaufort Sea coast. The section is mostly alluvium with little to no organic detritus (see Fig. 5.4), only unit E has some evidence of organic matter. RR-1 is approximately 200 cm long and 83 cm tall.

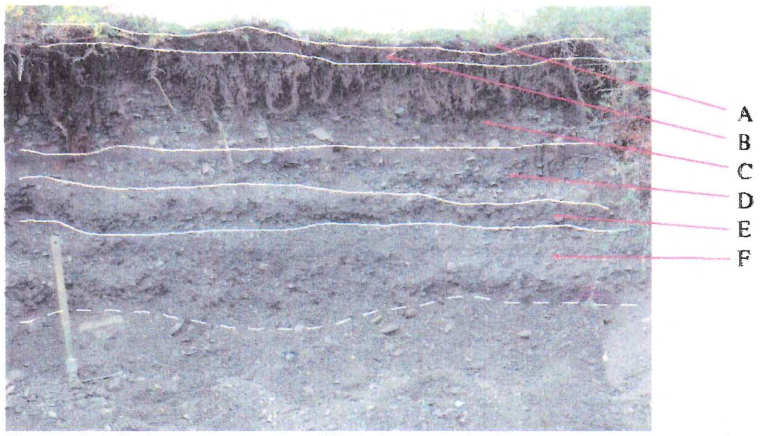

Figure 5.4 Sedimentary section RR-1 dug into the lowest most terrace in the Running River valley, illustrates multiple fining upwards sequences.

Unit (cm)	*Description of Section RR-1*
A. 0-3	-modern vegetation mat
	-mosses, shrubs, dwarf willow and dwarf birch
B. 3-9	-modern soil layer
	-peaty with fine to medium grained sand
	-light brown with large amounts of modern roots
C. 9-46	-flood couplet
	-top contact is not sharp, lower contact is sharp
	-fine unit ~10 cm thick, fine to coarse sand with some rare irregular shaped pebbles (0.5-1.5 cm diameter), with some modern root fragments
	-coarse unit ~27 cm thick, medium grained sand to cobbles that are poorly sorted, large grains are imbricated to roughly 30-40 degrees, and show a flow direction of 311-314 degrees orientation
	-no visible organic deposits
	-fining upwards sequence
	-grains are sub-angular to rounded in shape, but are random and have no preferred shape
D. 46-66	-flood couplet
	-fining upwards sequence
	-upper contact is sharp, lower contact is difficult to see
	-fine unit ~7 cm thick medium to very coarse sand, unit is more sorted than above unit, no organic detritus found
	-coarse unit ~13 cm thick coarse sand to large pebbles (1-4 cm in diameter) and rare large pebbles to cobbles (8-10 cm in diameter)
	-slight signs of imbrication, but difficult to measure
	-long axis of grains are oriented roughly parallel to bedding
	-no evidence of organic detritus through out the unit

Unit (cm)	*Description of Section RR-1*
E. 66-83	-poorly sorted unit, silt to cobble (5-6 cm diameter)
	-some evidence of imbrication of larger grains, orientation is difficult to determine
	-some small root fragment and other organic detritus
	-both upper and lower contacts are not clear
F. 83<	-flood couplet
	-fine layer 10-12 cm thick coarse sand to pea-gravel, some random large grains (1-3 cm in diameter), possible laminae (1 cm thick, 6-7 beds) defined by small fining upwards sequences
	-interpreted to be associated with one large flood event
	-no organic material
	-coarse unit (undetermined thickness) coarse, with a larger fine fraction compared to other coarse units in section
	-rare large pebbles (>15 cm in diameter), some degrees of imbrication, but grains are near horizontal

RR-2:

RR-2 was excavated near the mouth of the Running River where it enters the Beaufort Sea, and is 175 cm above the modern Running River channel and is approximately 200 cm wide and 92 cm high (see Fig. 5.5).

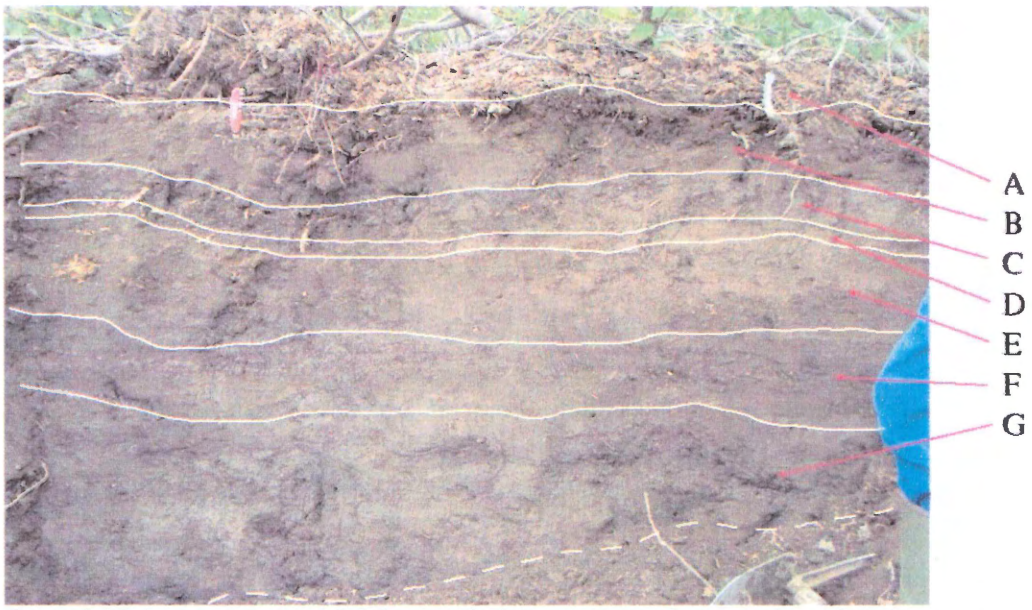

Figure 5.5 Sedimentary section RR-2 dug into the lowest terraces adjacent to the modern Running River channel, located near the mouth of the Running River (see Fig 5.1), illustrates multiple fining upwards sequences.

Unit (cm)	***Description of Section RR-2***
A. 0-1	-modern vegetation mat
	-surface has dead leaves, twigs and other plant matter
	-interpreted to have been deposited after the last major flood event
	-living plants: willow, mosses, grasses, and shrubbery

Unit (cm)	*Description of Section RR-2*
B. 1-13	-3 couplets of fine and coarse layers -1-1.5 cm thick beds -fine units are silty to fine sand with modern root fragments -coarse units are medium sand with organic balls and lenses composed of partly decomposed grass and leaf fragments that are orientated parallel to bedding
C. 13-24	-flood couplet -fine unit ~10cm thick fine silt with organic matter throughout the unit, some modern roots and no obvious structures of any kind -coarse unit ~1cm thick medium to coarse sand with no organic matter evident -sharp wavy contacts with adjacent units
D. 24-26	-flood couplet -fine unit ~1 cm thick silt to fine sand with some organic material -coarse unit ~1cm thick medium sand with no organic material -unit is very similar to unit C
E. 26-35	-flood couplet -fine unit ~3.5 -5 cm thick silt with lots of organic matter (leaf, grass and root fragments) -coarse unit ~3-4 cm thick fine to medium sand with lots of organic material in lenses, fragments of organic matter are indistinguishable
F. 35-57	-flood couplet -fine unit ~16 cm thick silt with organic matter -contact with above unit is sharp -organic layers and balls of plant material ~5cm depth in fine unit, are separated by fine beds (1 cm thick) -coarse unit ~4-7 cm thick medium to coarse sand -evidence of orange oxidation on lower contact that is not laterally extensive

Unit (cm)	*Description of Section RR-2*
G. 57<	-possible flood couplet, base of unit is beneath section in the ground
	-fine unit inter bedded with organic layers (0.2-0.5 cm thick) that are laterally extensive with possible ripple structures
	-contains orange oxidized balls ~2-3 cm diameter
	-some rare sticks and twigs that are orientated parallel to bedding, ~0.5 cm diameter

GFP:

GFP was excavated into the mouth of Grayling Creek where the modern Running River channel is eroding back into the mouth of Grayling Creek. Erosion into Grayling Creek by the Running River has exposed a cross section of the flood plain or delta exiting from Grayling Creek's mouth (see Fig 5.6). GFP is approximately 200 cm wide and 185 cm high.

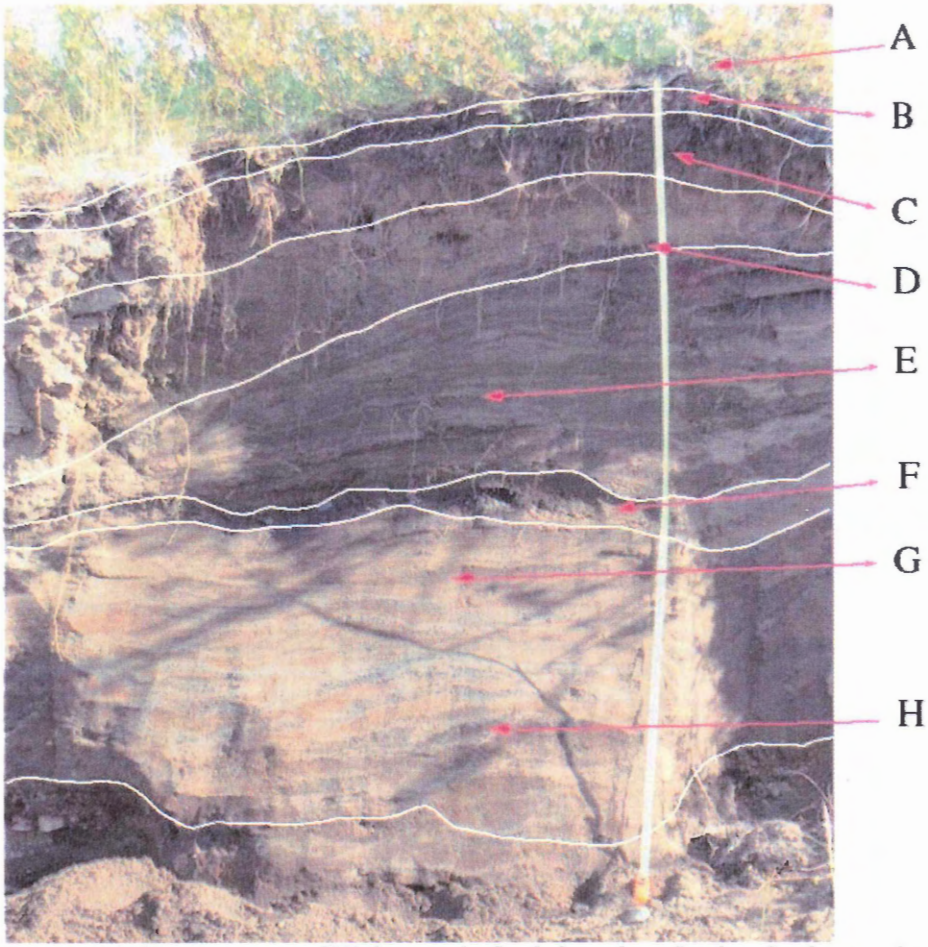

Figure 5.6 Sedimentary section GFP dug into the flood plain where Grayling Creek enters the Running River, illustrates two very coarse layers each of which is overlain by flaser bedding of clay-silt and fine sand.

Unit (cm)	***Description of Section GFP***
A. 0-5	-modern vegetation mat
	-dwarf willow, dwarf birch, grass, moss, Labrador tea, and other unknown shrubs
B. 5-11	-modern soil horizon, that contains modern roots and some silty material

Unit (cm)	*Description of Section GFP*
C. 11-28	-medium brown coloured silt to fine sand
	-contains some small pebbles, and traces of organic material (indistinguishable)
D. 28-43	-fine silt
	-beds in unit pinch and swell and is distinguished by orange oxidation between layers
	-unit contains some coarse material medium sand within oxidized layers
	-presence of organic remnants of grassy plant material
E. 43-117	-interpreted as a major flood package
	-unit is separated into two main sections -- a thick fine unit overlying a thinner coarse unit
	-fine unit is inter layered grey silt lenses that pinch and swell between layers of fine sand and clayey silt and extends down from 43 cm to 116 cm depth in the section, unit resembles flaser bedding
	-lenses are between 1-3 cm thick, clayey silt layers are between 1-2 cm thick, fine sand layers are between 1-2 cm thick
	-contacts between all layers are very sharp and there is evidence of orange oxidation between fine sand and clayey silt layers
	-presence of organic balls (3-4 mm diameter) between fine sand and clayey silt layers
	-coarse unit is poorly sorted coarse sand to fine pebbles and extends from 116-117 cm depth in the section
	-contacts are sharp both above and below the coarse unit
	-clasts or grains of unit appear to have some sort of varnish on them that is a dull grey colour and resembles graphite in its appearance

Unit (cm)	*Description of Section GFP*
F. 117-185	-interpreted as a major flood package
	-unit is separated into two main sections a thick fine unit overlaying a thinner coarse unit
	-fine unit is inter layered grey silt lenses that pinch and swell between layers of fine sand and clayey silt and extends down from 117 cm to 173 cm depth in the section, unit resembles flaser bedding
	-lenses are between 1-3 cm thick, clayey silt layers are between 1-2 cm thick, fine sand layers are between 1-2 cm thick
	-contacts between all layers are very sharp and there is evidence of orange oxidation between fine sand and clayey silt layers
	-presence of organic balls (3-4 mm diameter) between fine sand and clayey silt layers, organics are less frequent than unit E
	-sand layers are rusty red where colour is most pronounced between clayey silt and sand unit
	-contacts between beds are sharp and obvious
	-coarse sand in fine unit is poorly sorted with evidence of some bedding of coarse sand and sand to pebble layers that pinch and swell between 1-6 cm thickness
	-coarse unit is poorly sorted fine sand to large pebbles, with the occasional large clast (8-9 cm diameter)
	- clasts or grains of unit appear to have some sort of varnish on them that is a dull grey colour and resembles graphite in its appearance
	-contacts are sharp
G. 185<	-unit appears to be very similar to the fine flaser bedding of unit E and unit F, a clayey silt dominated unit

5.1.2 Channel Morphology Results

GPS surveys reveal numerous series of paired and unpaired cut and fill terraces along Grayling Creek. Terraces are bench like structures that represent past flood plains and are continuous on straight sections of the creek, and become discontinuous around sharp meanders. Relative terrace age increases in ascending order away from the modern channel resulting in young terraces occurring nearest the modern channel and the oldest terraces nearest to the top of the valley. Figure 2.9 illustrates the variety of terrace styles that occur in association with alluvial and fluvial systems. Terrace morphology changes in a down stream direction from relativity continuous paired cut and fill terraces, to less continuous unpaired cut and fill terraces, finally evolving into slip off terraces near the mouth of Grayling Creek. Terraces do not converge downstream, rather they seem to pinch out and terminate with new terraces forming in the downstream direction.

The youngest terraces on Grayling Creek P1 are paired cut and fill terraces that (see Fig. 5.8) remain for the majority of the survey length (~5 km) then becoming unpaired downstream between transects 20 and 19 (see Fig. 5.11). P1 remains unpaired until it terminates between transects 22 and 25.

Terraces A, B, C, D, E, and F are all discontinuous and can only be traced for a short distance. Each letter corresponds with a group of terraces that are unpaired, and on a specific side of Grayling Creek's modern channel. Figure 5.7 illustrates the extent of the GPS survey, and where each interpretation of valley morphology is located. Figure 5.8 shows a series of continuous and discontinuous cut and fill terraces. Terraces

designated an A correspond to the southern valley slope and terraces designated B are on the northern slope of the valley. Figure 5.9 exhibits continuations of A3 and of B2 terraces, and illustrates the commencement of a small discontinuous unpaired terrace, C1. Located between the southern P1 and C1 terraces there is a levee and flood plain (see Fig. 5.9). Figure 5.10 exhibits both continuations of A3 and P1, and the commencement of D1 and D2 terraces. Figure 5.11 show excellent continuations of D1 and D2, as well as P1 and A3. D3 is a newer terrace that appears between transect 15 and transect 17 and is therefore included with terraces designated D on the northern slope of Grayling Creeks valley. Discontinuous terraces E1 and E2 appear on the southern valley wall, where E1 is very short and terminates after a short distance. P1 terminates its southern terraces and turns into an unpaired terrace, however the northern terrace continues on. Figure 5.12 illustrates continuations of A3 on the southern valley wall and D1, D2, D3, and P1 on the northern valley wall. Figure 5.12 illustrates how Grayling Creek is met by a tributary containing terraces designated F. F1, F2, and F3 that represent the start of a conversion of terrace types from a cut and fill style to the slip off terrace style. The tributary meeting Grayling Creeks main channel is dry, and has no surface flow, as seen in August 2005 during field study, climatically the rainiest month (Environment Canada 2004). Slip off terraces dominate Grayling Creek's river valley for the last 1.5 km of the creek, until it meets the Running River. Grayling Creek's channel has slipped off and incised in a northerly direction (see Fig 5.7) causing a steep slope to the north and a gradual stepping of terraces to the south.

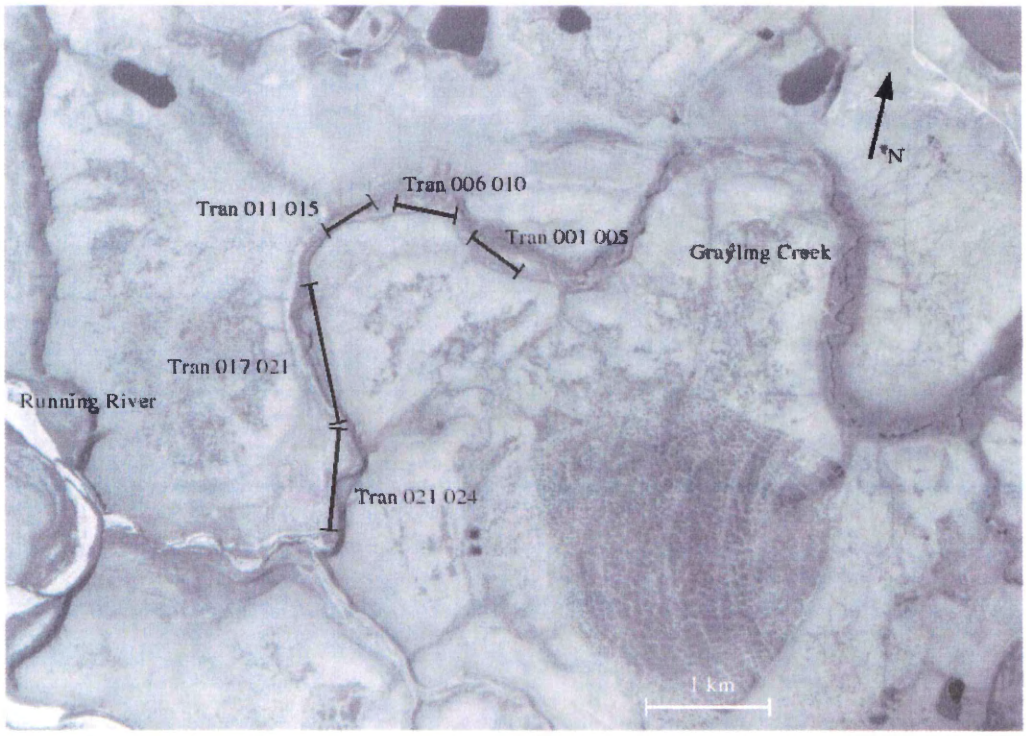

Figure 5.7 Air photo of Grayling Creek (NAPL 1985) illustrating the locations and extent of each channel morphology interpretation of Grayling Creek.

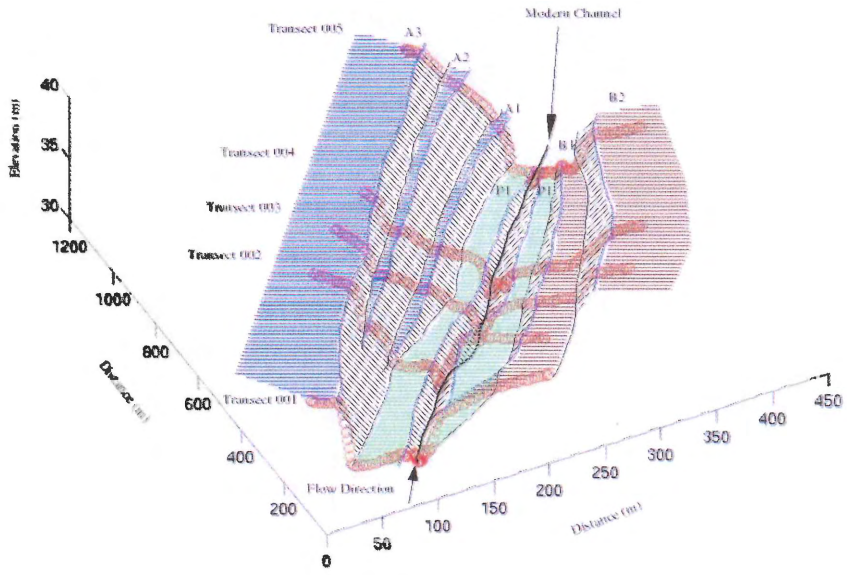

Figure 5.8 Transects 001 to 005, illustrating one set of paired terraces (P1) and multiple unpaired terraces (A and B). Red circles represent points of GPS surveys.

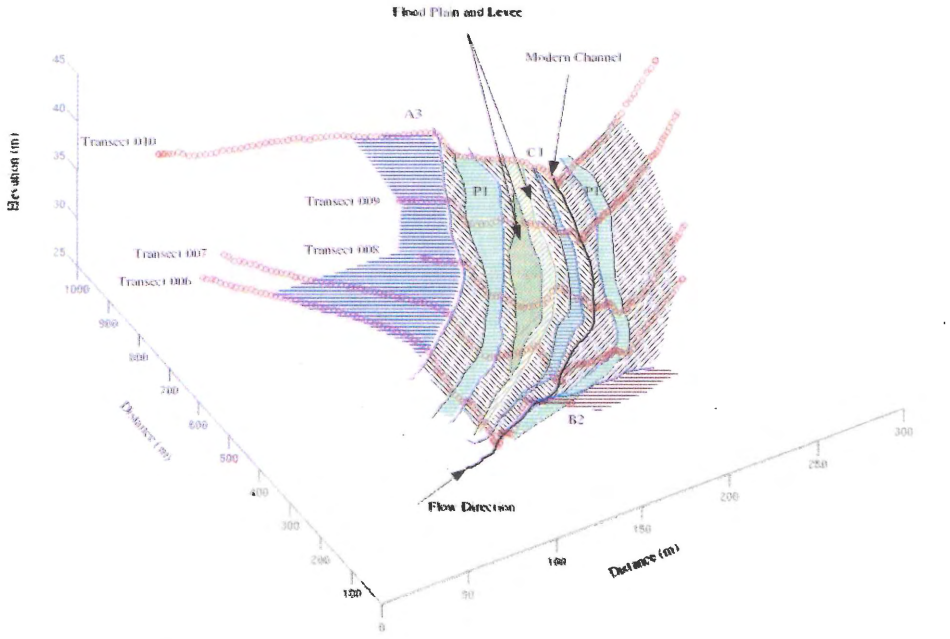

Figure 5.9 Transects 006 to 010, illustrating continuation of the sole paired terrace (P1) and termination of unpaired terraces (B), unpaired terraces (A1 and A2 also have terminated, however A3 continues through the section. Unpaired terrace C initiates and terminates within the section and is associated with a flood plain and a levee.

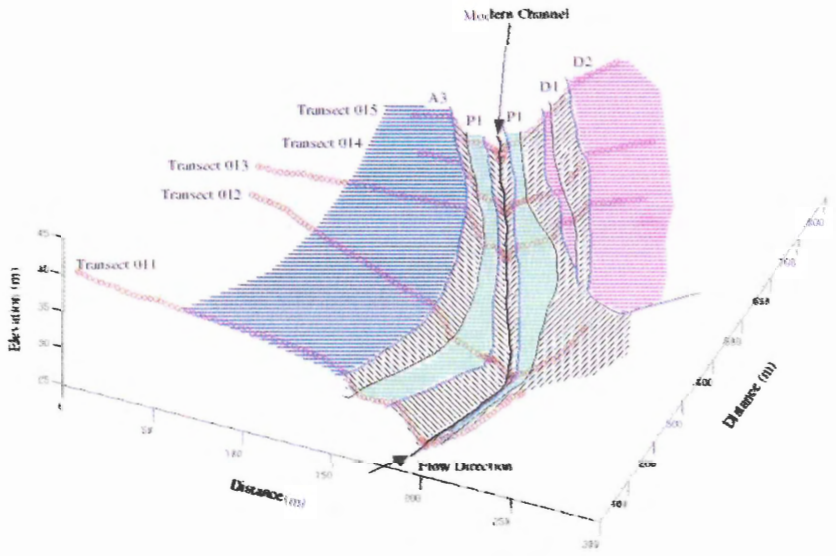

Figure 5.10 Transects 011 to 015, illustrating the continuation of A3 and P1, and the initiation of D unpaired terraces.

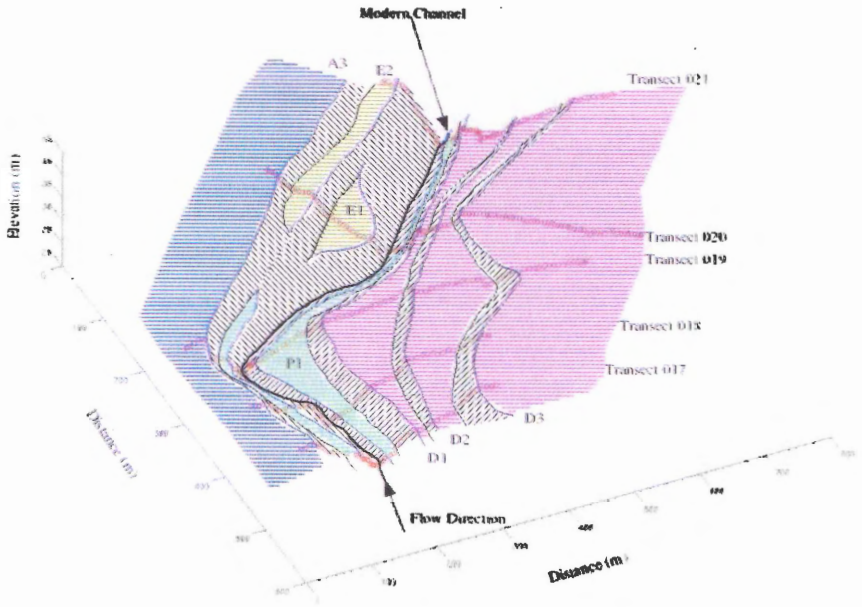

Figure 5.11 Transects 017 to 021, illustrating the continuation of A3 and D unpaired terraces, and the initiation of E unpaired terraces. P1 becomes unpaired part of the way through the section and is now only seen on the north valley wall.

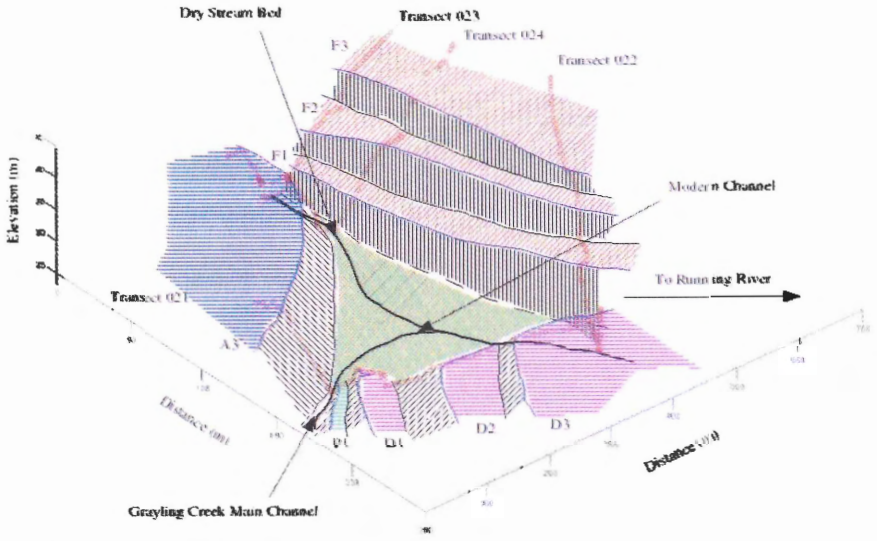

Figure 5.12 Transects 021 to 024, illustrating the junction of Grayling Creek's main channel and a dry bedded tributary, with multiple unpaired terraces (F terraces) comparable in size to Grayling Creek's terraces.

5.1.3 Hydrology Results

Parameter	*Flow 1: Matchsticks*	*Flow 2: Matchsticks*	*Flow 1: Manning*	*Flow 2: Manning*
Slope (S)	0.0050	0.0025	0.005	0.0025
Hydraulic Radius (R)	0.1768	0.3123	0.1768	0.3123
Velocity (m/s)	0.4275	0.3055	0.6020	0.6220
Flow Rate (m^3/s)	0.1550	0.3972	0.2182	0.8086

Table 5.1 Results from flow analysis on Grayling Creek calculated by both matchstick and Manning equation calculations.

Discharge Source	*Snow Depth at Melt*	*Time (days)*	*Volume (m^3)*	*Discharge (m^3/s)*
Grayling Creek Freshet	average snow depth	7	4.2×10^5	0.69
	maximum snow depth	7	8.6×10^5	1.42
	average snow depth	14	4.2×10^5	0.35
	maximum snow depth	14	8.6×10^5	0.71

Table 5.2 Results for discharge from Grayling Creek.

Discharge Source	*Time (days)*	*Volume (m^3)*	*Discharge (m^3/s)*
Bigwok Basin	1/2	4.8×10^6	110.7
	1	4.8×10^6	55.3
	2	4.8×10^6	27.7

Table 5.3 Results for drainage discharges from Bigwok Basin (using similar drainage durations to findings by Mackay 1981, and Marsh & Neumann 2001)

Discharge Source	*Discharge (m^3/s)*	*Channel With (m)*	*Stream Power (J/s)*
Grayling Creek Current	0.39	3.25	4.41
Grayling Creek Freshet	0.69	3.25	7.81
	1.42	3.25	16.1
	0.35	3.25	3.96
	0.71	3.25	8.04
Bigwok Basin	110.7	40.0	101.8
	55.3	40.0	50.9
	27.7	40.0	25.5

Table 5.4 Stream power results for Grayling Creeks freshet assuming that flow never exceeds the limits of current channel width (3.25m), and Bigwok Basin assuming a channel width that incorporates the total flood plain width of Grayling Creek (75.0m).

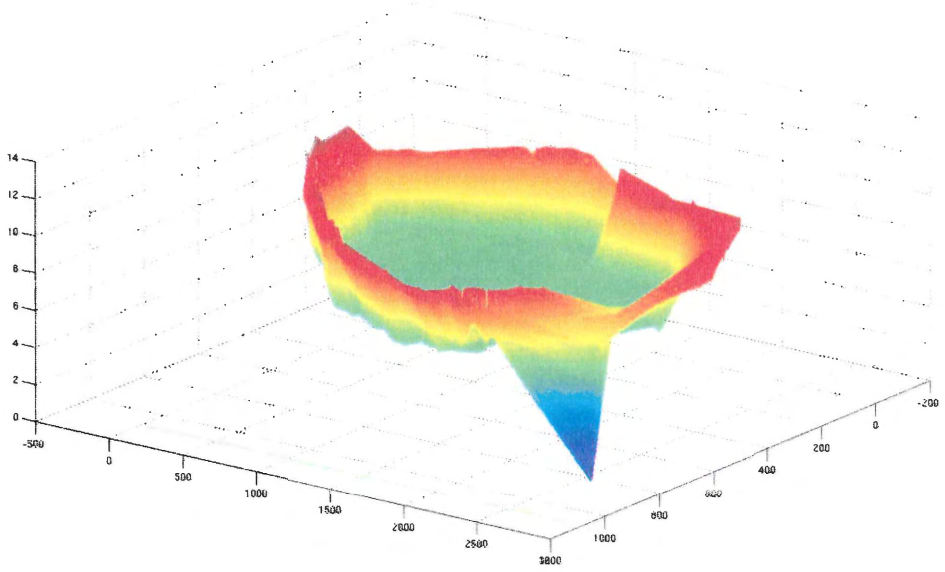

Figure 5.13 Bathymetric depiction of Bigwok Basin and its drainage channel, where the base of the lake in the figure represents the current lake level in Bigwok Basin illustrating the total drained volume in Bigwok Basin.

5.1.4 Volume of a Thaw Lake (Bigwok Basin)

Bigwok Basin is a partially drained thaw lake, with two distinct past lake levels that can be observed in air photos and field observations. A large drainage channel links Bigwok Basin to the Running River, and represents the location of the topographic low that Bigwok tapped and drained into (see Fig 5.13). Bigwok Basin has a total drained volume of 6.4543×10^6 m^3. The first drainage event drained 4.7805×10^6 m^3 of water, initiating and incising a drainage channel into the Running River. The second drainage event produced a drainage volume of 1.6738×10^6 m^3 of water, that too flowed into the Running River through the same drainage channel. Both of these flood events are large and would produce a massive flux of water into the Running River compared to the normal volume of flow occurring daily in the river.

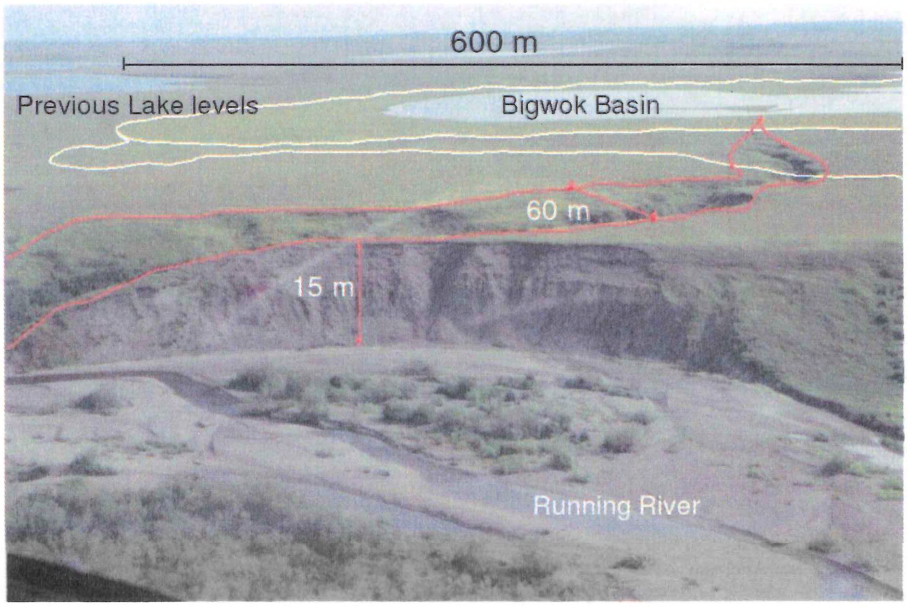

Figure 5.14 Photo of Bigwok Basin indicating where previous lake levels have been, and drainage channel into the Running River.

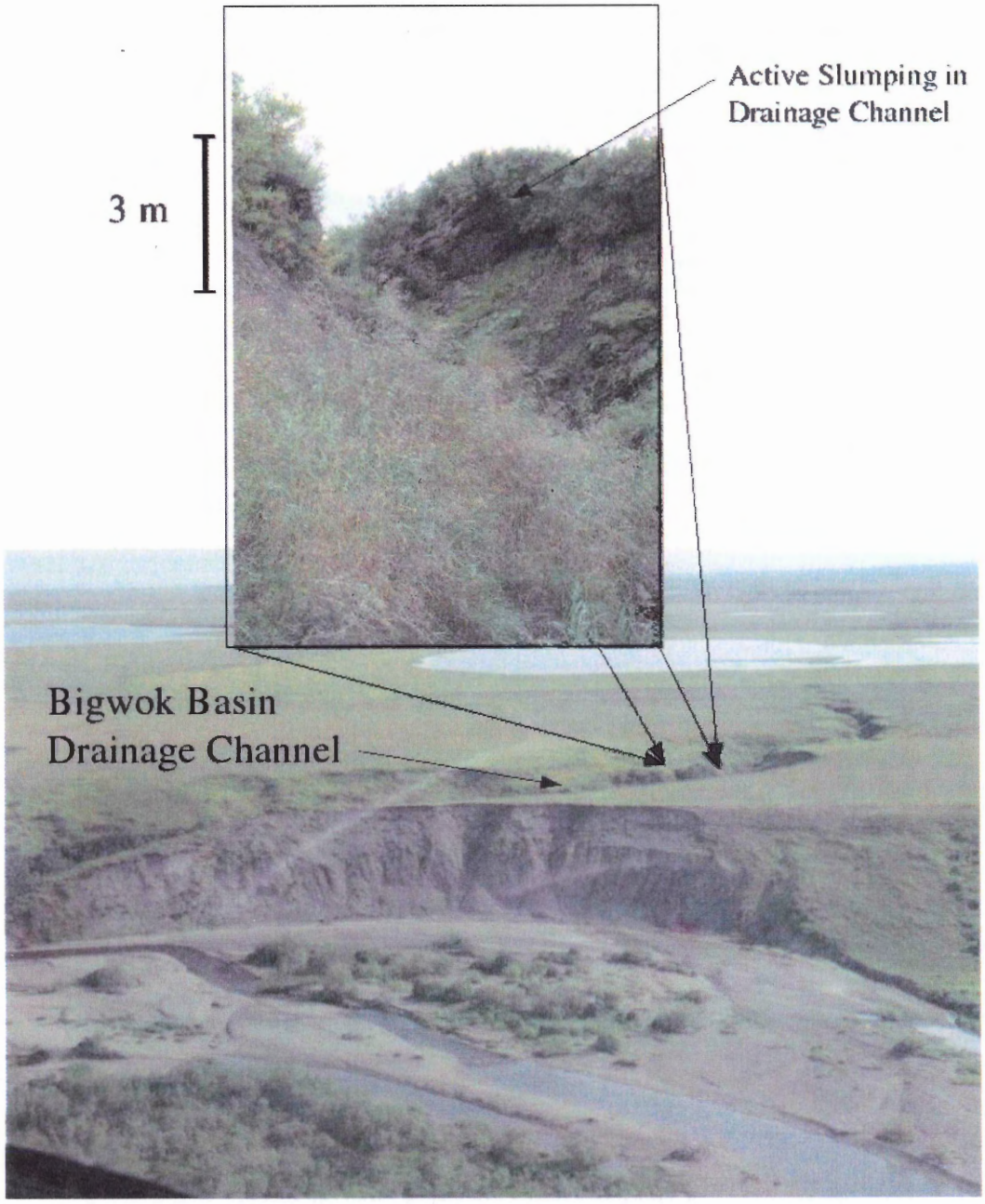

Figure 5.15 Photo indicating the active slumping occurring presently on Bigwok Basin's drainage channel.

5.1.5 Grayling Creek Drainage Basin

The drainage basin of Grayling Creek has a total area of approximately 12.3 km^2 (see Fig. 5.16 and 5.17). From this area, an estimate can be made for the average freshet drainage volume and a fifty year maximum freshet drainage can be calculated. Grayling Creek experiences a spring freshet (thaw flood) each year, usually between April and May, where on average 34.0 cm of snow melts over a period of weeks. Under the assumption of a very rapid spring freshet calculations indicate that if an average snow depth of 34.0 cm (Environment Canada 2004) melts and drains, 4.2×10^5 m^3 would drain into Grayling Creek. If a fifty year maximum of 70.0 cm (Environment Canada 2004) snow depth melts in the same rapid manner Grayling Creek would experience 8.6×10^5 m^3 of water into its channel each year.

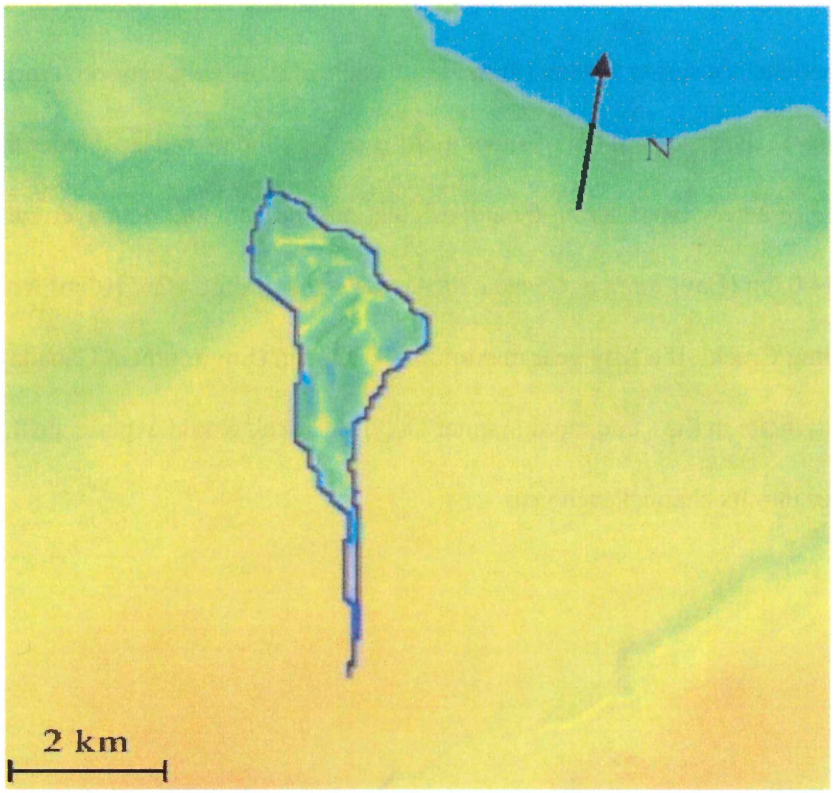

Figure 5.16 Grayling Creeks drainage basin calculations from RiverTools (RIVEX 2004).

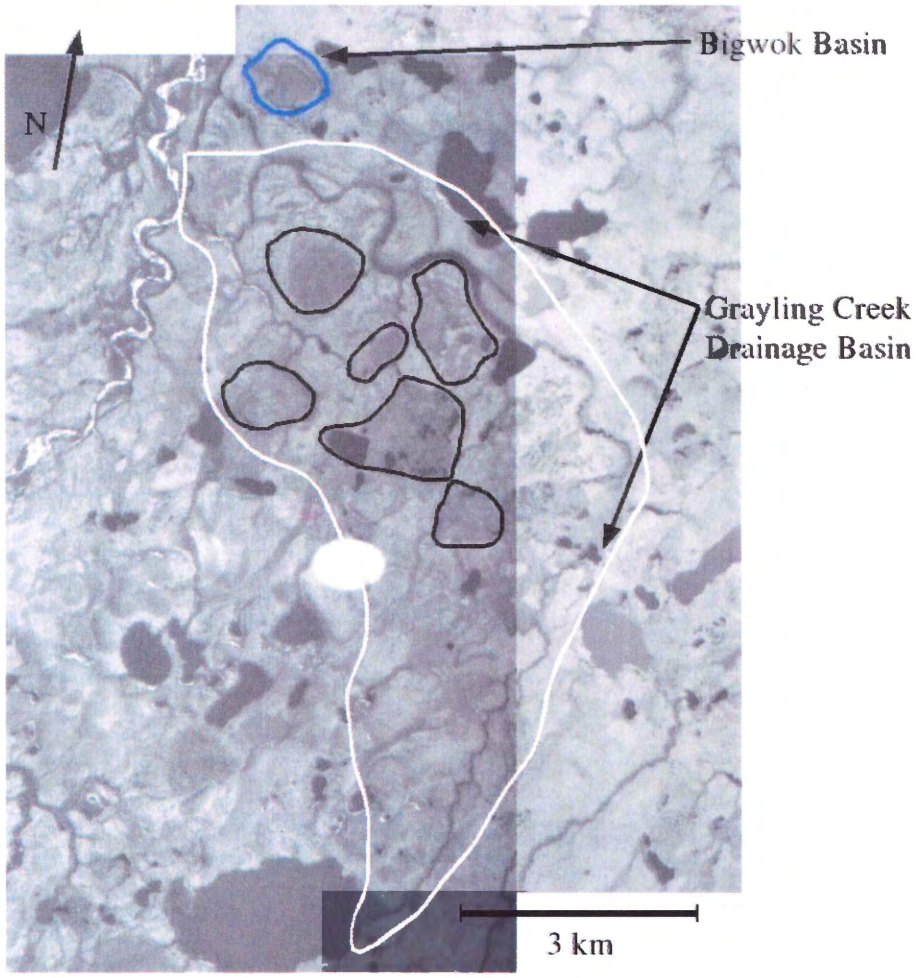

Figure 5.17 Air Photo (NAPL 1985), drained thaw lakes that have affected Grayling Creek are outlined inside of the drainage basin, and then can be compared to Bigwok Basin located.

5.2 Discussion

5.2.1 Sedimentary Analysis

Six sedimentary sections excavated into paired and unpaired cut and fill terraces in Grayling Creek and the Running River show multiple flood deposits. In each of the four sedimentary sections GC-1, GC-2. GC-3, and GFP from Grayling Creek layered flood deposits consisting of a lower coarse unit overlain by a fine slack water deposit were discovered. Similar flood deposits were discovered in the two Running River sections RR-1 and RR-2. From these sedimentary analyses into terraces on the Running River and Grayling Creek interpretations indicate that multiple flooding events have occurred on the Running River and more importantly on Grayling Creek. Large flood packages are interpreted as possible thaw lake drainage events, where a thaw lake has catastrophically drained into Grayling Creek. Thinner flood deposits most likely are not from thaw lake drainage events, they could be a result of large freshet (spring thaw) flood years. Sedimentary deposits are interpreted to be of flood origin because there is no evidence of cross bedding, if there were evidence of cross bedding the deposits could be interpreted to be from point bar/ channel migration.

One sample from GC-3 was sent away to Beta Analytic in Florida for radio carbon dating, however the date was erroneous and came back young (a negative age). We conclude this to be a result of modern carbon, possibly from modern roots or humic acids alluvating downwards through soil horizons. Erroneous dates are a result of

alterations in atmospheric carbon ratios, caused by nuclear weapons testing in the 1950's.

5.2.2 Channel Morphology

Terrace formation commonly is attributed to either base level drop or up-lifting topography. Both result in downward incision of the channel into underlying material. Another mechanism is increases in stream power. In thaw lake regions, rapid incision and formation of terraces may be caused by catastrophic drainages of thaw lakes. However the Yukon Coastal Plain has been tectonically stable since before the Quaternary and has been affected by repeated glaciations, the latest of which occurred roughly 120 000 years ago during the Buckland glacial sequence (Rampton 1982). The Yukon Coastal Plain was not affected by the last glacial maximum 20 000 years ago.

Grayling Creek is a small stream, overfit by its valley with well developed terrace sequences. Presence of an over fit valley indicate that some other mechanism other than modern stream activity is affecting channel and valley morphology.

Streams seen on other Arctic coastal plains comparable in size to Grayling Creek did not exhibit the same over fit valley. Thaw lakes dominate the coastal plain landscape and are a major process in shaping the surficial evolution of the landscape. Thaw lake drainages are high energy events and are capable of displacing large amounts of sediment resulting in large amounts of incision (Mackay 1981, Marsh & Neumann 2001). Bigwok Basin illustrates the amount of potential energy stored in every expanding thaw lake. It is therefore very plausible that the terraces and over fit valley of Grayling Creek are a result of multiple catastrophic thaw lake drainage events that have occurred within Grayling

Creek's drainage basin. Each event incising downwards in to the current flood plain resulting in the many well formed terraces present in Grayling Creek.

5.2.3 Hydrology Measurements

Using the Manning equation an average velocity was calculated for the dimensional measurements on Grayling Creek Flow 1 and Flow 2 (see Table 5.1). All flow rate estimates are less than 1.0 m^3/s but are broadly variable There is relatively little flow within Grayling Creek. All measurements conducted on Grayling Creek occurred in August climatically the rainiest month. When rain falls do occur Grayling Creek's resultant hydrograph spike would be short lived and relatively small, due to the small size of Grayling Creeks drainage basin. Grayling Creeks drainage basin will be presented and discussed later in this chapter.

Discharge results (see Table 5.2 and 5.3) indicate that drainage of Bigwok Basin has a significantly greater discharge than the maximum spring freshet that occurs in Grayling Creek. Furthermore, stream power results indicate that a drainage like Bigwok Basin into Grayling Creek has significantly more power than a maximum freshet event (see Table 5.4). From these two indications is obvious that a thaw lake drainage unleashed into Grayling Creek of similar size to Bigwok Basin has more potential to erode and remove material. If Bigwok Basin drained in a ½ day it would produce 101.8 J/s of stream power, if it drained in 2 days it would produce a stream power of 25.5 J/s. These are impressive numbers especially when compared to the maximum stream power produced by the annual freshet in Grayling Creek. If 70.0 cm of snow melted in 7 days

16.1 J/s of stream power is produced. It is comparable to Bigwok Basin's drainage occurring over 2 days, however once the channel width is taken into account and compared significant differences become obvious. Freshet calculations used a channel width of 3.25 m representative of the current channel width. Bigwok Basin's drainage stream power is calculated using the entire flood plain width (40.0 m). Even with significant differences in channel width, Bigwok Basin's drainage event is significantly larger than the annual freshet in Grayling Creek.

Grayling Creek's valley is much too large for the size and strength of the current stream in place that has 4.41 J/s of stream power. Evidence from flow measurements on Grayling Creek indicate that in order for a valley the size of Grayling Creek to have formed, flow rates must have been significantly greater to have caused the large amounts of incision. Modern flow rates in Grayling Creek are not sufficient to produce the resultant valley. Thaw lake floods have sufficient stream power to cause large amounts of incision.

5.2.4 Volumetric Analysis of Bigwok Basin

Bigwok Basin is a drained thaw lake, and it appears through changes in vegetation and paleo shoreline (see Fig. 5.14) evidence that it did so in two massive drainage events. Calculated flood discharges from two lakes in the Northwest Territory indicate that a combination of thermal and physical processes are responsible for channel initiation and incision (Marsh & Neumann 2001, Mackay 1981). Lake Illisarvik one of the studied lakes is located on Richards Island, approximately 60 km west of Tuktoyaktuk, N.W.T.

and was artificially drained in the 1970's (Mackay 1981, 1986, 2002). It had an initial lake volume of roughly 3.0 x 10^5 m^3 (Mackay 1981) a volume an order of magnitude lower than either of the drainage volumes produced by Bigwok Basin. Lake drainage was on the order of ½ a day on Illisarvik and where rapid drainage produced large amounts of incision (Marsh & Neumann 2001, Mackay 1981, 1988). Bigwok Basin was not artificially drained, however once natural drainage commenced it most likely drained in a similar fashion to the much smaller lake Illisarvik. Except that total volume was greater and discharge likely larger because the drainage gradient is larger for Bigwok Basin compared to Lake Illisarvik (15 m drop in elevation for Bigwok Basin vs. 4-6 m drop in elevation for Illisarvik (Mackay 1981)). This accounts for the large amounts of incision produced when Bigwok Basin was tapped and drained into the Running River (see Fig 5.13).

There is a question as to why there are two apparent drainage events from Bigwok Basin. In both of the lakes studied in the Northwest Territories once drainage was initiated the lake either empties completely, or drains to its current lake level (Marsh and Neumann 2001, Mackay 1981). However from air photos it can be observed that many drained lake basins on Arctic coastal plains and lowlands show multiple paleo shorelines. I propose two hypotheses for multiple shorelines. Firstly, the lake did indeed drain completely, and then refilled and drained again. This is difficult to produce because of the presence of the incised drainage channel. It would seem very probable that any more water coming into the lake basin would simply drain out thorough the drainage channel

that has incised in a headward direction into the current lake. The second method involves a blockage of flow through the drainage channel. In ice rich permafrost the ice content decreases after a few (1.0- 4.0 m) meters depth, therefore the ground is less and less sensitivity to thermal erosive properties of the drainage event (see Fig 5.18 A). Instead physical erosion would play a larger role in the removal of material. Once drainage incision has reached through the ice-rich layer, expansion and widening can occur more readily because of the lower latent-heat content of the ground. This results in a tunnelling effect with an overhanging block. Eventually the force of gravity would overcome the tensile strength of the over hanging block of ice rich material (see Fig.5.15), and a resultant slump block would detach from the channel bank and slide into and potentially blocking the drainage channel (see Fig. 5.18 B). If the slump block is of sufficient size to halt drainage, it may cause the lake to again stabilize and recommence margin erosion. Once stabilized the lake could then develop new shorelines, accounting for the obvious vegetation and elevation differences observed at paleo-shorelines.

5.2.5 Grayling Creek Drainage Basin

The drainage volume of Bigwok is at least one order of magnitude larger than the maximum spring thaw flood experienced on Grayling Creek in the last fifty years. Figure 5.16 and 5.17 indicate that at least six thaw lakes that are comparable in area to Bigwok with drainage channels leading into Grayling Creek have drained. Although exact volumes of these lakes are unknown it is reasonable to assume that they had a volume of water comparable to Bigwok Basin. Therefore Grayling Creek has been affected by at

least six drainage events in approximately the last 10'000 years, and most likely has been affected by more drainage events whose lakes are not as obvious from air photos.

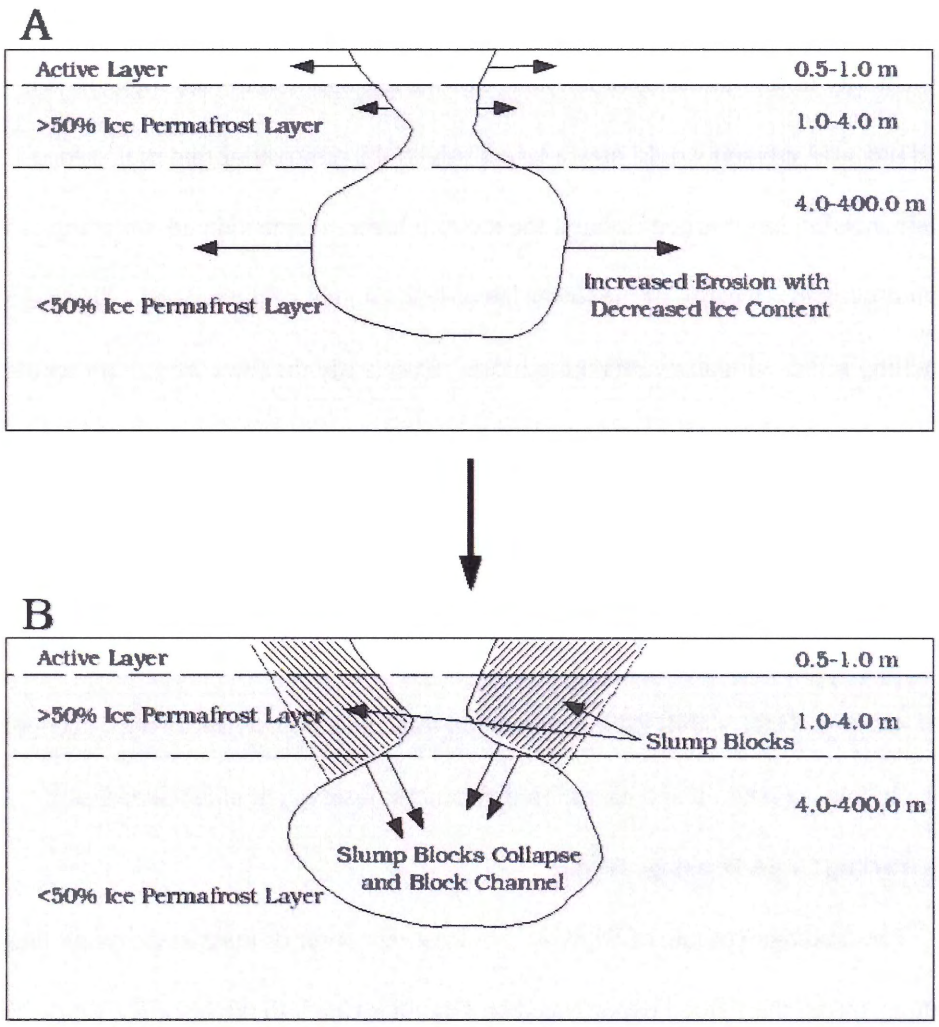

Figure 5.18 Diagrams indicating hypothesised drainage channel evolution towards slope collapse and channel blockage. Figure A. Diagram indicating the relative amounts of erosion estimated by vector arrows. Figure B. Diagram indicating the formation and collapse of slump blocks in a drainage channel.

5.6 General Discussion:

Grayling Creek is a lower order stream that is situated in an over fit valley. Its modern channel is small and unable to cause the large amounts of sediment removal required for Grayling Creek's large valley. From the results it is evident that sedimentary records of flood deposits are present and indicate that floods occur and affect Grayling Creek. However drainage channels produced during thaw lake drainage have small amounts of deposition and large amounts of incision, removal and transport of material (Brewer et al. 1993). These characteristics are evident in the drainage channel from Bigwok Basin and possibly explain Grayling Creek's over fit valley.

The Yukon Coastal Plain is characteristically a dry arid region that experiences the majority of annual water flow in rivers during the spring freshet. One thaw lake drainage event have a volume at least one order of magnitude larger than the total volume of spring melt. Discharges from thaw lake floods are 20 to 100 times (see Tables 5.2 and 5.3) more than freshest discharges, and stream power is 2 to 5 times more powerful.

Thaw lake drainage events initiate channels by overwhelming and over saturating the active layer resulting in open water flow (Mawer 2005). Once overland flow occurs rapid incision results and erodes quickly through the peat dominated active layer. Thaw lake drainages like Bigwok Basin occur in any ice rich permafrost locality. Since these lake drainage events are so substantial and large compared to the annual snow melt flood thaw lakes present a solution to the presence of large post glacial valleys on the Yukon Coastal Plain and other Arctic coastal plains.

Evidence from fining upwards sequences are consistent with some deposition occurring during drainage events and spring thaw flood events. However the amount of deposition is minimal during a lake drainage when compared to the volume of material removed by peak flow incision. Bigwok illustrates consequences of high stream power during the floods, large amounts of sediment removed during lake carving, a 15.0 m deep by 500 m long channel to the Running River with no evidence of deposition except for post flood slumping. Power of the flood through Grayling Creek probably is less than for the Bigwok Basin event, because channel gradient is less and width is greater, both of which decrease shear stress of the river bed. However, six drained lake basins exist around and within the Grayling Creek drainage basin, and each exhibits one or multiple channels cutting into Grayling Creek (see Fig. 5.17). Surface area of these lakes are similar to Bigwok Basin, so volumes possibly are comparable (within an order of magnitude) to the volume drained from Bigwok Basin. It is therefore reasonable to assume that when each of these drainage events occurred the flood volumes would have be very similar to Bigwok Basins drainage volume. Each drainage event sent a massive surge of water into and down Grayling Creek in a relatively instantaneous amount of time (1-2 days). According to previous findings in the North West Territories, Canada (Marsh & Neumann 2001, Mackay 1981) lakes drain with in a matter of hours to days. Each event would have discharge and stream power far larger than the largest freshet, causing rapid amounts of incision.

Base level drop is an alternative hypothesis for the formation of channel terraces

found on Grayling Creeks valley walls. However the area has been tectonically stable for a considerable amount of time. This area also has not been ice covered for approximately the last 100'000 years and was unaffected by the last glacial maximum, being situated in the ice free corridor between the Laurentide and Cordilleran ice sheets. Small local ice caps in the Barn and Richardson Mountains probably would not cause significant Holocene age isostatic adjustment on melting. Grayling Creek is most likely of early Holocene to Late Pleistocene age, and therefore negates the possibility that Grayling Creek is a glacial out washing feature on the Yukon Coastal Plain.

It therefore seems probable that Grayling Creek's terraces formed by multiple catastrophic lake drainage events rather than through the gradual incision produced by it's underfit stream. Each tapping and drainage would produce a very large flood easily capable of incising into Grayling Creek's valley floor. Even though terrace formation is attributed to thaw lake drainages, it is not possible to estimate the number of drainage events from channel terraces due to their discontinuous nature. Terraces pinch-out and commence for the entire length of Grayling Creek. It is likely that individual flood events incise terraces, but also are dependent on location of lake tapping.

Chapter 6: Conclusions and Future Work

Previous to this study thaw lakes and river networks have been viewed as separate processes acting independently of one another on the landscape, and Arctic river networks were thought to be dominated by freshet flood discharges in spring. However, my measurements from the Yukon Coastal Plain suggest that this view should be reconsidered for low to intermediate order river channels in regions with thaw lakes. Freshet floods do indeed result in large volumes of water travelling through river channels in a short period of time. However thaw lake drainages may result in discharges 20 to 100 times greater, and may recur, on every 10^2 to 10^3 years. The amount of energy created during thaw lake drainage events is sufficient to melt ice rich permafrost, initiating channel incision in Arctic river drainage networks (Marsh & Neumann 2001).

Thaw lake drainages have been observed from a few localities in Northern Canada, where lake drainage created enough energy to rapidly melt permafrost, resulting in rapid incision and channel formation. Evidence of rapid thaw lake drainage illustrated by Bigwok Basin results in rapid melting and incision of ice rich permafrost forming a large drainage channel. Grayling Creek has experienced at least six large drainage events comparable in size to the floods from Bigwok Basin. All likely occurred during the Holocene, because this has been the period of significant thermokarst development. Sedimentary analysis conducted on Grayling Creek and the Running River produce

evidence of flood deposits in multiple fining upwards sequences. Fining upwards sequences are interpreted as being individual flood deposits.

Previous work has always attributed the morphology and formation of Arctic river channels to the flood experienced each spring where snow and ice run off increase flow through river networks. Channel morphology of Grayling Creek is wide compared to the modern stream resulting in the stream being over fit. Channel terraces occur in paired and unpaired terrace couplets, caused by episodic down cutting events. Terrace formation traditionally is due to base level drop, however this has not occurred in this region since the last glacial sequence, therefore insinuating that Grayling Creek is of Holocene age. Moreover, even with base level drop, Grayling Creek has insufficient stream power to incise the observed depth. Freshets do attribute to some channel morphology, however channels are not likely to be altered as significantly by these flood events. Modern stream power in Grayling Creek for the majority of the year is non existent due to the extensive winter months, and in the summer stream flow is minimal. In contrast, thaw lake drainages produce relatively massive flood events and last for a very short period of time. Bigwok Basin illustrates the drainage potential of a thaw lake, channel dimensions indicate rapid incision and removal of material does occur during thaw lake drainages.

Future work is required to better understand the circumstances surrounding thaw lake drainage events. This thesis has investigated the magnitude of thaw lake discharges and shown that thaw lake drainages are massive events that affect channel initiation and

morphology in the Running River watershed. However several questions remain unanswered, including: 1. Is Grayling Creek typical or atypical of intermediate-order streams in thaw lake dominated landscapes? My methods should be extended to other channels, and to other thaw lake regions on Earth. 2. What is the precise chronology of drainage events? This question might be addressed by dating of drained lake basins to construct flood chronology for selected drainage basin; 3. What sedimentological markers are characteristic of thaw lake flood events, compared to freshets? This question might be addressed by comparing, for example micro and macro fossil assemblages in lake muds with slack water flood deposits.

Observations from the Yukon Coastal Plain show intermediate order streams may be predominantly formed, incised, and develop cross grading due to thaw lake dynamics. If this is the case, channels may be expected to change significantly if current changes in high latitude climate drive, for example, more rapid thaw lake expansion. This lends urgency to investigating the relationship between thaw lakes and rivers.

References:

Ashmore, P., and Church, M. 2001. The Impact of Climate Change on Rivers and River Processes in Canada, Report Bulletin 555, Geological Survey of Canada.

Black, R.F. 1976. Periglacial Features Indicative of Permafrost, Ice and Soil Wedges. Quaternary Research, **6**: 3 -26.

Brewer, M.C., Carter, L.D., Glenn, R. 1993. Sudden Drainage of a Thaw Lake on the Alaskan Arctic Coastal Plain. *In* Sixth International Conference on Permafrost Proceedings. Beijing, China. South China University Press, Vol.1, pp. 48-53.

Burn, C.R. 1992. Recent Ground Warming Inferred from the Temperature in Permafrost near Mayo, Yukon Territory. Geological Survey of Canada, **Paper 65-36**.

Dixon, J. 1996. Cretaceous and Tertiary. *In* The Geology Mineral and Hydrocarbon Potential of Northern Yukon and North-western District of Mackenzie. Geologic Survey of Canada, Bulletin 422. pp. 301-317.

Dyke, L.D. 1996. White, Barn, and Campbell Uplifts. *In* The Geology, Mineral and Hydrocarbon Potential of Northern Yukon Territory and North-western District of Mackenzie. Geological Survey of Canada, Bulletin 422. pp. 333-357.

Environment Canada 2004. Climate Data of Shingle Point A (1957-2004), Environment Canada.

Fetter, C.W. 2001. Applied Hydrogeology. Prentice Hall Inc., Upper Saddle River, New Jersey, pp. 33 -53.

French, H. 1996. The Periglacial Environment. Addison Wesley Longman Limited, Edinburgh.

GeoBase 2004. CDED Modified USGS Format Maps. GeoBase.

Harris, S.A. 2002. Causes and Consequences of Rapid Thermokarst Development in Permafrost of Glacial Terrain. Permafrost and Periglacial Processes, **13**(3): 237-242.

IPA 2004. Global Permafrost Distribution. International Permafrost Association.

Leopold, L.B., Wolman, M.G., and Miller, J.P. 1995. Fluvial Processes in Geomorphology. Dover Publications Inc., New York.

Mackay, J.R. 1981. An Experiment in Lake Drainage, Richards Island, Northwest Territories, A Progress Report. *In* Current Research Part A, Geological Survey of Canada, Paper 81-1A: 63-68.

Mackay, J.R. 1986. The First Seven Years (1978 -1985) of Ice Wedge Growth, Illisarvik Experimental Drained Lake Site, Western Arctic Coast, Canada. Canadian Journal of Earth Sciences, **23**(11): 1782 -1795.

Mackay, J.R. 1986. The Permafrost Record and Quaternary History of North-western Canada, Correlation of Quaternary Deposits and Events Around the Margin of the Beaufort Sea: Contribution from a Joint Canadian-American Workshop, Report Open File 1237, Geological Survey of Canada.

Mackay, J.R. 1988. Catastrophic Lake Drainage, Tuktoyaktuk Peninsula Area, District of Mackenzie. *In* Current Research Part D, Geological Survey of Canada, Paper 88-1D: 83-90.

Mackay, J.R., and Burn, C.R. 2002. The First 20 Years (1978 to 1998 -1999) of Ice Wedge Growth at the Illisarvik Experimental Drained Lake Site, Western Arctic Coast, Canada. Canadian Journal of Earth Sciences, **39**(1): 95 -111.

Marsh, P., and Neumann, N.N. 2001. Processes Controlling the Rapid Drainage of Two Ice-rich Permafrost -Dammed Lakes in NW Canada. Hydrological Processes, **15**: 3433-3446.

McDonald, B.C., and Lewis, C.P. 1973. Geomorphic and Sedimentologic Processes of Rivers and Coast, Yukon Coastal Plain., Report 73 -39, Terrain Sciences Division Geological Survey of Canada.

Miall, A.D. 1992. Alluvial Deposits. *In* Facies Models. Geological Association of Canada. pp. 119 -143.

Mawer, A.S. 2005. Permafrost-controlled Break in Fractal Scaling of River Networks, Yukon Coastal Plain, Western Canadian Arctic, Honours Thesis. pp.. 1-80.

Murton, J.B. 1996. Thermokarst-lake-basin Sediments, Tuktoyaktuk Coastlands, Western Arctic Canada. Sedimentology, **43**: 737 -760.

Norris, D.K. 1996. Physiographic Setting. *In* The Geology, Mineral and Hydrocarbon Potential of Northern Yukon Territory and North-western District of Mackenzie. Geological Survey of Canada, Bulletin 422. pp. 7-19.

NRCAN 2004. Distribution of Permafrost in Canada. Geological Survey of Canada.

Rampton, V.N. 1982. Quaternary Geology of the Yukon Coastal Plain, Report Bulletin 317, Geological Survey of Canada.

Ritter, D.F., Kochel, R.C., and Miller, J.R. 2002. Process Geomorphology. McGraw -Hill Higher Education, New York.

RIVEX 2004. RiverTools Topographic and River Network Analysis. RIVEX LLC.

Selby, M.J. 1985. Earth's Changing Surface. Oxford University Press, Oxford.

Trenhaile, A.S. 2004. Geomorphology A Canadian Perspective. Oxford University Press, Toronto.

Williams, P.J., and Smith, M.W. 1989. The Frozen Earth Fundamentals of Geocryology. Cambridge University Press, New York.

Woo, M.K., and Sauriol, J. 1981. Effects of Snow Jams on Fluvial Activities in the High Arctic. Physical Geography, **2**: 83 -89.

Appendix A: The Quaternary Geology of the Yukon Coastal Plain, surrounding the Running River Area (Rampton 1982).

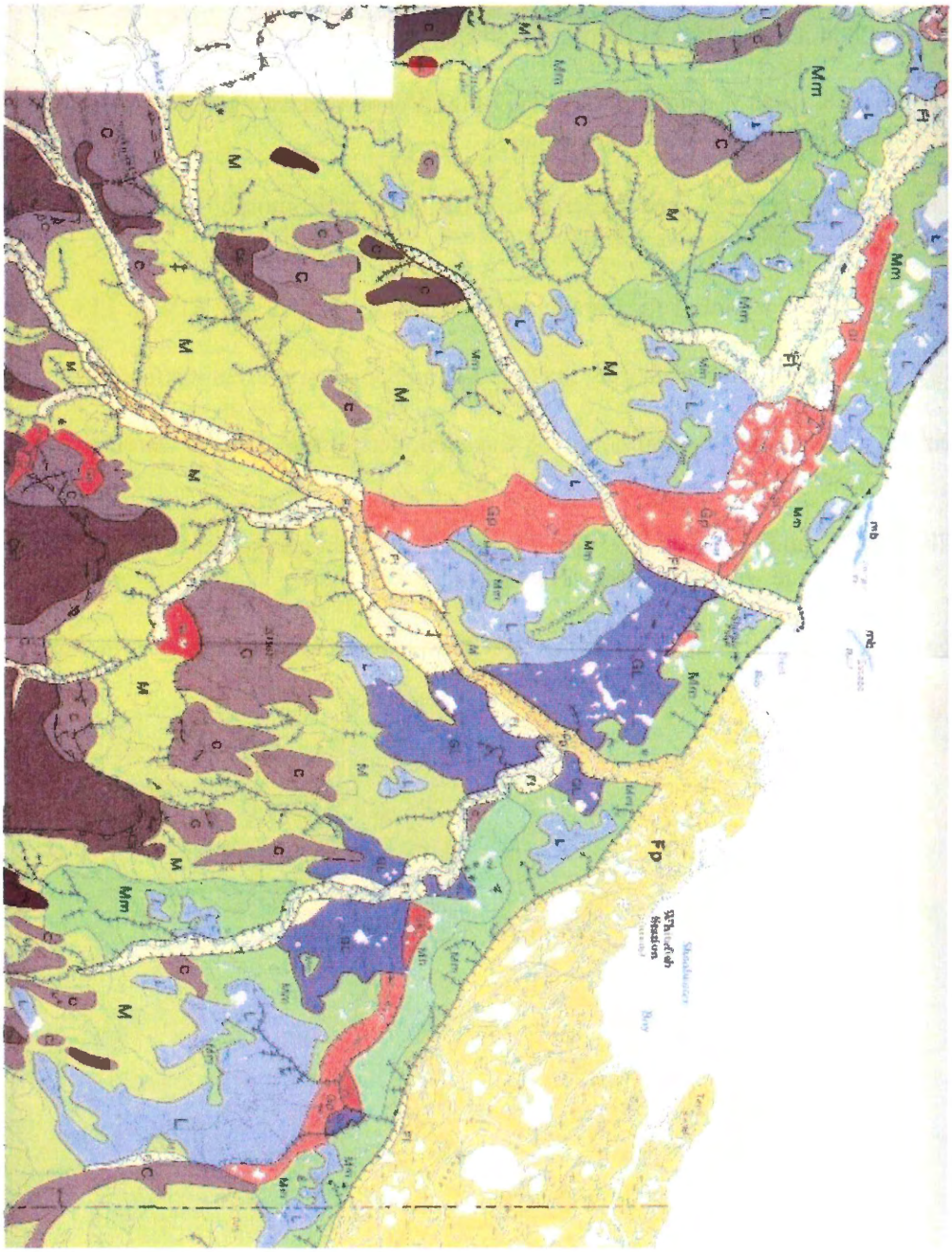

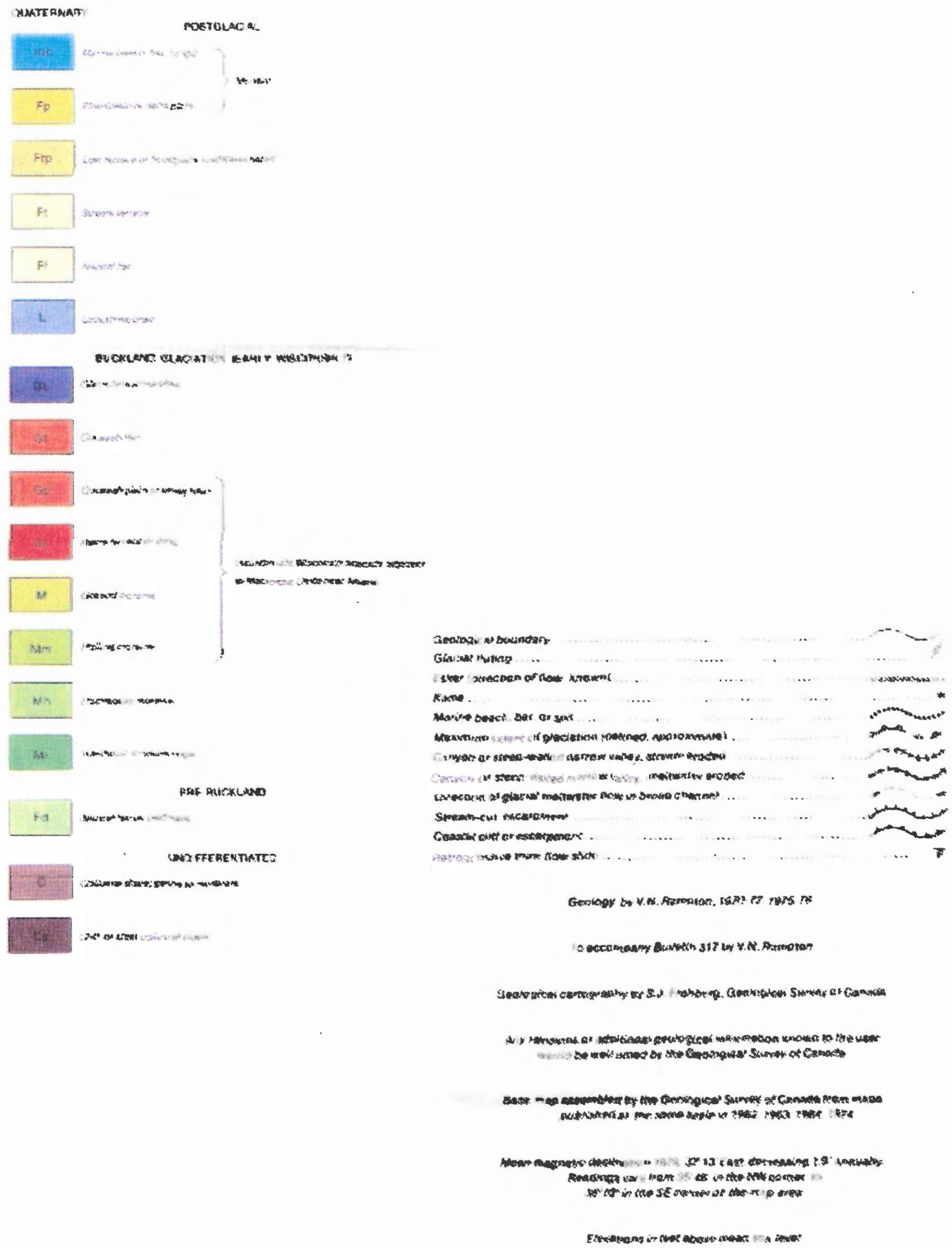
QUATERNARY
POSTGLACIAL
Fp
Ftp
Ft
L
BUCKLAND GLACIATION (EARLY WISCONSIN?)
M
Mm
PRE-BUCKLAND
UNDIFFERENTIATED
Geological boundary
Marine beach, bar, or spit
Stream-cut escarpment
Coastal cliff or escarpment
To accompany Bulletin 317 by V.N. Rampton
Elevations in feet above mean sea level

Appendix B: Results of drainage basin analysis of Grayling Creek from RiverTools (RIVEX 2004).

DATA SUMMARY FOR patched River BASIN

Prune type = Order, Threshold = 2.00000

BASIN AREA (km)^2

Order	Number	Minimum	Maximum	Range	StdDev.	Average
1	76	1.86846E-002	7.05974E-001	6.87289E-001	1.05848E-001	1.11883E-001
2	18	1.30689E-001	1.77346E+000	1.64277E+000	3.82613E-001	4.37499E-001
3	6	4.42035E-001	2.19119E+000	1.74915E+000	6.76042E-001	1.36869E+000
4	1	1.23412E+001	1.23412E+001	0.00000E+000	0.00000E+000	1.23412E+001

TOTAL CHANNEL LENGTH (km)

Order	Number	Minimum	Maximum	Range	StdDev.	Average
1	76	6.70307E-002	5.40110E+000	5.33407E+000	8.44597E-001	7.14814E-001
2	18	7.23932E-001	1.34711E+001	1.27472E+001	3.05156E+000	3.23193E+000
3	6	2.44206E+000	1.80873E+001	1.56453E+001	5.77087E+000	1.00053E+001
4	1	8.24581E+001	8.24581E+001	0.00000E+000	0.00000E+000	8.24581E+001

LONGEST CHANNEL LENGTH (km)

Order	Number	Minimum	Maximum	Range	StdDev.	Average
1	76	6.70307E-002	5.40110E+000	5.33407E+000	8.44597E-001	7.14814E-001
2	18	4.94793E-001	8.05660E+000	7.56181E+000	1.70856E+000	2.09600E+000
3	6	1.41558E+000	1.08478E+001	9.43225E+000	3.21671E+000	4.29581E+000
4	1	1.47107E+001	1.47107E+001	0.00000E+000	0.00000E+000	1.47107E+001

MAGNITUDE

Order	Number	Minimum	Maximum	Range	StdDev.	Average
1	76	1	1	0	0.00000E+000	1.00000E+000
2	18	2	7	5	1.58016E+000	2.94444E+000
3	6	4	14	10	3.07770E+000	8.16667E+000
4	1	76	76	0	0.00000E+000	7.60000E+001

STRAIGHT-LINE LENGTH (km)

Order	Number	Minimum	Maximum	Range	StdDev.	Average
1	76	6.68337E-002	5.20559E+000	5.13876E+000	8.16246E-001	6.86983E-001
2	18	9.27643E-002	3.00519E+000	2.91243E+000	7.48956E-001	8.84768E-001
3	6	1.14280E-001	2.61034E+000	2.49606E+000	7.86561E-001	1.07283E+000
4	1	3.51069E+000	3.51069E+000	0.00000E+000	0.00000E+000	3.51069E+000

ALONG-CHANNEL LENGTH (km)

Order	Number	Minimum	Maximum	Range	StdDev.	Average
1	76	6.70307E-002	5.40110E+000	5.33407E+000	8.44597E-001	7.14814E-001
2	18	9.29563E-002	3.30619E+000	3.21324E+000	8.03963E-001	9.43432E-001
3	6	1.14552E-001	2.79123E+000	2.67668E+000	8.45512E-001	1.17640E+000
4	1	4.09209E+000	4.09209E+000	0.00000E+000	0.00000E+000	4.09209E+000

ELEVATION DROP (m)

Order	Number	Minimum	Maximum	Range	StdDev.	Average
1	76	1.00000E+000	3.30000E+001	3.20000E+001	7.62026E+000	7.22368E+000
2	18	1.00000E+000	2.30000E+001	2.20000E+001	6.40312E+000	8.66667E+000
3	6	0.00000E+000	3.90000E+001	3.90000E+001	1.36433E+001	1.61667E+001
4	1	2.00000E+001	2.00000E+001	0.00000E+000	0.00000E+000	2.00000E+001

STRAIGHT-LINE SLOPE

Order	Number	Minimum	Maximum	Range	StdDev.	Average
1	76	1.65846E-003	3.49913E-002	3.33328E-002	7.32597E-003	1.24074E-002
2	18	1.34206E-003	2.62406E-002	2.48985E-002	7.33993E-003	1.28382E-002
3	6	0.00000E+000	2.53554E-002	2.53554E-002	8.50778E-003	1.29008E-002
4	1	5.69689E-003	5.69689E-003	0.00000E+000	0.00000E+000	5.69689E-003

ALONG-CHANNEL SLOPE

Order	Number	Minimum	Maximum	Range	StdDev.	Average
1	76	1.65504E-003	3.49083E-002	3.32532E-002	7.08147E-003	1.19550E-002
2	18	1.26894E-003	2.61784E-002	2.49094E-002	7.16546E-003	1.20403E-002
3	6	0.00000E+000	2.40896E-002	2.40896E-002	8.14032E-003	1.19654E-002
4	1	4.88748E-003	4.88748E-003	0.00000E+000	0.00000E+000	4.88748E-003

NUMBER OF LINKS

Order	Number	Minimum	Maximum	Range	StdDev.	Average
1	76	1	1	0	0.00000E+000	1.00000E+000
2	18	1	6	5	1.28260E+000	1.72222E+000
3	6	1	6	5	1.80278E+000	2.50000E+000
4	1	19	19	0	0.00000E+000	1.90000E+001

TRIBS. OF 1 ORDER LOWER

Order	Number	Minimum	Maximum	Range	StdDev.	Average
1	76	0	0	0	0.00000E+000	0.00000E+000
2	18	0	5	5	1.58016E+000	9.44444E-001
3	6	0	1	1	3.72678E-001	1.66667E-001
4	1	4	4	0	0.00000E+000	4.00000E+000

TRIBS. OF 2 ORDERS LOWER

Order	Number	Minimum	Maximum	Range	StdDev.	Average
1	76	0	0	0	0.00000E+000	0.00000E+000
2	18	0	0	0	0.00000E+000	0.00000E+000
3	6	0	5	5	1.70783E+000	1.50000E+000
4	1	5	5	0	0.00000E+000	5.00000E+000

TRIBS. OF 3 ORDERS LOWER

Order	Number	Minimum	Maximum	Range	StdDev.	Average
1	76	0	0	0	0.00000E+000	0.00000E+000
2	18	0	0	0	0.00000E+000	0.00000E+000
3	6	0	0	0	0.00000E+000	0.00000E+000
4	1	13	13	0	0.00000E+000	1.30000E+001

NETWORK DIAMETER (LINKS)

Order	Number	Minimum	Maximum	Range	StdDev.	Average
1	76	1	1	0	0.00000E+000	1.00000E+000
2	18	2	7	5	1.28260E+000	2.72222E+000
3	6	3	11	8	2.67187E+000	6.16667E+000
4	1	30	30	0	0.00000E+000	3.00000E+001

BASIN RELIEF (km)

Order	Number	Minimum	Maximum	Range	StdDev.	Average
1	76	1.00000E-003	3.30000E-002	3.20000E-002	7.62026E-003	7.22368E-003
2	18	3.00000E-003	3.70000E-002	3.40000E-002	1.00100E-002	1.82778E-002
3	6	1.10000E-002	7.60000E-002	6.50000E-002	2.24400E-002	3.73333E-002
4	1	9.40000E-002	9.40000E-002	0.00000E+000	0.00000E+000	9.40000E-002

SINUOSITY

Order	Number	Minimum	Maximum	Range	StdDev.	Average
1	76	1.00207E+000	1.27615E+000	2.74082E-001	4.61588E-002	1.03762E+000
2	18	1.00207E+000	1.33116E+000	3.29087E-001	8.54335E-002	1.07286E+000
3	6	1.00238E+000	1.32089E+000	3.18506E-001	1.08394E-001	1.08778E+000
4	1	1.16561E+000	1.16561E+000	0.00000E+000	0.00000E+000	1.16561E+000

DRAINAGE DENSITY (1/km)

Order	Number	Minimum	Maximum	Range	StdDev.	Average
1	76	1.35573E+000	1.47128E+001	1.33571E+001	2.69528E+000	5.97786E+000
2	18	4.15302E+000	1.06591E+001	6.50612E+000	1.77793E+000	7.15554E+000
3	6	5.37503E+000	8.35429E+000	2.97926E+000	1.23821E+000	6.87894E+000
4	1	6.68152E+000	6.68152E+000	0.00000E+000	0.00000E+000	6.68152E+000

SOURCE DENSITY (km)^-2

Order	Number	Minimum	Maximum	Range	StdDev.	Average
1	76	1.41648E+000	5.35200E+001	5.21035E+001	1.13959E+001	1.62583E+001
2	18	3.94709E+000	1.72103E+001	1.32632E+001	4.17079E+000	8.87693E+000
3	6	4.10737E+000	1.35736E+001	9.46622E+000	3.26461E+000	7.31014E+000
4	1	6.15822E+000	6.15822E+000	0.00000E+000	0.00000E+000	6.15822E+000

Average Along-channel Link Lengths

Order	Number	Avg. (km)
1	76	0.715
2	31	0.548
3	15	0.471
4	19	0.215

Average Straight-Line Link Lengths

Order	Number	Avg. (km)
1	76	0.687
2	31	0.523
3	15	0.439
4	19	0.206

Appendix C: Flow and Velocity Measurements from Grayling Creek.

Flow 1: Time (s) to travel 2 m	*Flow 1: Velocity (m/s)*	*Flow 2: Time (s) to travel 2 m*	*Flow 2: Velocity (m/s)*
3.95	0.51	7.42	0.27
4.06	0.49	6.31	0.32
4.77	0.42	6.33	0.32
4.91	0.41	6.46	0.31
5.03	0.4	6.84	0.29
4.60	0.43	5.98	0.33
4.61	0.43	6.53	0.31
4.53	0.44	6.83	0.29
5.13	0.39	7.17	0.28
4.85	0.41	6.49	0.31
4.39	0.46	7.37	0.27
4.50	0.44	6.09	0.33
4.87	0.41	7.65	0.26
4.67	0.43	6.29	0.32
4.92	0.41	6.27	0.32
5.03	0.4	6.08	0.33
4.52	0.44	6.65	0.3
4.46	0.45	6.50	0.31
5.06	0.4	6.24	0.32
5.28	0.38	6.30	0.32